EXPRESSIVE AND RECEPTIVE LANGUAGE AREAS DETERMINED BY A NON-INVASIVE RELIABLE METHOD USING FUNCTIONAL MAGNETIC RESONANCE IMAGING AND MAGNETOENCEPHALOGRAPHY

Kyousuke Kamada, M.D., Ph.D.
Department of Neurosurgery,
The University of Tokyo,
Tokyo, Japan

Yutaka Sawamura, M.D., Ph.D.
Department of Neurosurgery,
Hokkaido University,
Sapporo, Japan

Fumiya Takeuchi, Ph.D.
Research Institute for Electric Science,
Hokkaido University,
Sapporo, Japan

Shinya Kuriki, Ph.D.
Research Institute for Electronic Science,
Hokkaido University,
Sapporo, Japan

Kensuke Kawai, M.D., Ph.D.
Department of Neurosurgery,
The University of Tokyo,
Tokyo, Japan

Akio Morita, M.D., Ph.D.
Department of Neurosurgery,
The University of Tokyo,
Tokyo, Japan

Tomoki Todo, M.D., Ph.D.
Department of Neurosurgery,
The University of Tokyo,
Tokyo, Japan

Reprint requests:
Kyousuke Kamada, M.D., Ph.D., and
Tomoki Todo, M.D., Ph.D.,
Department of Neurosurgery,
The University of Tokyo,
7-3-1 Hongo, Bunkyo-ku,
Tokyo 113-8655 Japan.
Email: kamady-k@umin.ac.jp

Received, March 23, 2006.
Accepted, October 13, 2006.

OBJECTIVE: It is known that functional magnetic resonance imaging (fMRI) and magnetoencephalography (MEG) are sensitive to the frontal and temporal language function, respectively. Therefore, we established combined use of fMRI and MEG to make reliable identification of the global language dominance in pathological brain conditions.

METHODS: We investigated 117 patients with brain lesions whose language dominance was successfully confirmed by the Wada test. All patients were asked to generate verbs related to acoustically presented nouns (verb generation) for fMRI and to read three-letter words for fMRI and MEG.

RESULTS: fMRI typically showed prominent activations in the inferior and middle frontal gyri, whereas calculated dipoles on MEG typically clustered in the superior temporal region and the fusiform gyrus of the dominant hemisphere. A total of 87 patients were further analyzed using useful data from both the combined method and the Wada test. Remarkably, we observed a 100% match of the combined method results with the results of the Wada test, including two patients who showed expressive and receptive language areas dissociated into bilateral hemispheres.

CONCLUSION: The results demonstrate that this non-invasive and repeatable method is not only highly reliable in determining language dominance, but can also locate the expressive and receptive language areas separately. The method may be a potent alternative to invasive procedures of the Wada test and useful in treating patients with brain lesions.

KEY WORDS: Expressive language function, Functional magnetic resonance imaging, Language dominance, Magnetoencephalography, Receptive language function

Neurosurgery 60:296-306, 2007 DOI: 10.1227/01.NEU.0000249262.03451.0E www.neurosurgery-online.com

Brain asymmetries have been of considerable interest in neurology for more than a century. Based on clinicopathological studies, the "classical mode" of language organization consists of a frontal "expressive" area for planning and executing speech and writing, and a temporal "receptive" area for analysis and identification of linguistic sensory stimuli. This basic scheme of language functions has generally been accepted, with the assumption that both expressive and receptive functions dominantly exist in the same hemispheric side.

The Wada test has been considered the most reliable method to determine language dominance. According to one of the largest studies performed to date, 4 and 96% of right-handed subjects with chronic epilepsy have speech dominance in the right and left hemispheres, respectively (3). Furthermore, several studies suggested the possibility of atypical language representation in patients with chronic epilepsy (20–30%) (9, 28). However, the procedure of successive anesthetization of each hemisphere by intracarotid injections of sodium amobarbital requires catheterization and irradiation. Furthermore, the Wada test results can only demonstrate a relative distribution of language functions across the two hemispheres. More detailed information on localization of specified language functions within a hemisphere is important for understanding the language networks, as well as the treatment of brain lesions.

The use of functional magnetic resonance imaging (fMRI) has recently been developed to identify the hemisphere with language dominance. Most language fMRI studies have observed activations in the inferior frontal gyrus (IFG) and middle frontal gyrus (MFG) using tasks such as word generation and categorization (16, 24, 29). Detection of the receptive language area by fMRI has been reported to be more difficult than that of the expressive language function, and the use of listening or sentence comprehension tasks has resulted in visualization of only a few pixels in the temporoparietal region (8, 16, 25, 26). In addition, a fundamental limitation of an fMRI-based brain mapping is the varying degrees of regional hemodynamic responses under pathological brain conditions (7, 10, 15). Therefore, a clinical interpretation of localized activations on fMRI remains complicated and controversial.

Magnetoencephalography (MEG) reflects intracellular electric current flow in the brain and allows accurate localization of the current dipole sources. Dipoles of MEG deflections that peaked at approximately 400 milliseconds after word presentation (late responses) have been observed to localize in the temporoparietal regions. These late responses have been considered to be related to the receptive language function (19, 20). We have also observed dense dipole clusters of the semantic late responses in the superior temporal gyrus (STG), supramarginal gyrus (SmG), and fusiform gyrus (FuG) of the suspected dominant hemisphere (11, 12). Therefore, we sought to use MEG not only as an additional diagnostic tool for identifying the language dominance, but also to localize the receptive language center.

In the present study, we describe a non-invasive method to locate the expressive and receptive language areas by co-utilizing fMRI and MEG. The language dominance determined by our method matched the results from the Wada test with 100% accuracy. The usefulness of the method was well demonstrated, especially in those patients who showed dissociated expressive and receptive language functions. The data show that this method is highly reliable and may be useful in the management of patients with brain lesions as well as in studying normal brain functions.

METHODS

Patients

The functional brain mapping using fMRI (with the verb generation task) and MEG was performed in 117 patients with brain lesions since August 1999 (>7 yr) after this project was approved by the Institutional Committee for Ethics (*Table 1*). fMRI studies with the abstract/concrete (A/C) categorization task were also performed in 106 patients. Ninety-seven patients also underwent the Wada test to confirm the dominant cerebral hemisphere for language functions. Six patients showed negative Wada test results owing to the steal effect of a large arteriovenous malformation (AVM) or an overdose. The final analyses were performed in 87 patients (48 men, 39 women), who underwent Wada test, fMRI, and MEG investigations. The mean age (± standard deviation) was 43.6 ± 14.1 years. The Edinburgh Handedness Inventory was used to estimate the patients' handedness (18). A written informed consent was obtained from the patient or his/her family before participation in the study.

Magnetic Resonance Protocols

Anatomic magnetic resonance imaging (MRI) and fMRI were performed during the same session with a 1.5-T whole-body magnetic resonance scanner with echo-planar capabilities and a standard whole-head transmit-receiver coil (Siemens Vision, Erlangen, Germany). During the procedures, foam cushions were used to immobilize the head.

Language fMRI

The patients were instructed to respond to all language tasks silently. fMRI data was acquired with a T2-weighted echo-planar imaging sequence (echo time, 62 ms; repetition time, 114 ms; flip angle, 90 degrees; slice thickness, 4 mm; slice gap, 2 mm; field of view, 260 mm; matrix, 64 × 128; 14 slices). Each fMRI session consisted of three dummy scan volumes followed by three activation and four baseline (rest) periods. During each period, five echo-planar imaging volumes were collected, yielding a total of 38 imaging volumes and 2 minutes 32 seconds in measurement time for each session. fMRI data of language-related semantic responses were acquired as follows. All subjects were examined with two different lexical semantic language paradigms; verb generation by listening to nouns and A/C categorization by reading words. All words for semantic tasks were selected from common Japanese words listed in the electronic dictionary of the National Institute for Japanese Language.

Verb Generation Task

For the auditory stimuli (duration ranges were between 400 and 600 ms), common concrete nouns spoken by a native Japanese speaker with a flat intonation were recorded and digitized with a sampling rate of 44,000 Hz. A backward playback of the sound files (reference sounds) was used to eliminate the primary auditory activation during the rest periods with the same inter-stimuli intervals (1600–2400 ms) as the active periods. The auditory stimuli were delivered binaurally via two 5-m-long plastic tubes terminating at a headphone. The sound intensity was approximately 95 dB sound pressure level at the subject's ear. Subjects were instructed to silently generate a verb related to each presented noun during the active periods and passively listen to the reference sounds during the rest periods.

A/C Categorization Task

Visual stimuli were presented on a liquid crystal display monitor with a mirror above the head coil allowing the patients to see the stimuli. Words consisting of three *Kana* letters (Japanese phonetic symbols) were presented in a 300-millisecond exposure time with interstimuli intervals ranging from 2800 to 3200 milliseconds. Patients were instructed to categorize the presented word silently into "abstract" or "concrete" based on the

TABLE 1. Summary of patients' brain lesions types[a]

	Glioma	Chronic Epilepsy	AVM	Meningioma	Cavernous malformation	Cerebral ischemia	Total
fMRI with VG + MEG	44	39	18	6	4	6	117
fMRI with A/C	41	34	15	6	4	6	106
Amytal test	42	29	16	6	4	0	97
Final analyses	39	26	12	6	4	0	87

[a] AVM, arteriovenous malformation; fMRI, functional magnetic resonance imaging; VG, verb generation task; MEG, magnetoencephalography; A/C, abstract/concrete categorization task.

nature of the word. During interval periods, patients passively viewed random dots of destructured *Kana* letters that were controlled to have the same luminance as the stimuli to eliminate primary visual responses.

Before scanning, all patients had a brief practice time, and the fMRI examinations were repeated for each task to confirm the reproducibility. After data acquisition, a motion detection program (MEDx; Medical Numerics, Sterling, VA) discarded fMRI sessions containing motion artifacts exceeding 25% of the pixel size. A Gaussian spatial filter (6 mm in half width) was applied, and functional activation maps were calculated by estimating the Z-scores between the rest and activation periods using Dr. View (Asahi Kasei, Tokyo, Japan). Pixels with Z-scores higher than 2.2 ($P < 0.05$) were considered to indicate real activation and were used for mapping. Image distortion of fMRI was corrected by maximizing the mutual information of the fMRI data sets and three-dimensional T1-weighted MRI (3D-MRI) scans of the patient's brain (morphing compensation). The result from each fMRI session was co-registered with the 3D-MRI by the Affine transformation (5). After total number of the activated pixels in the IFG and MEG were automatically counted, a patient was considered to have unilateral language dominance when hemispheric pixels of one hemisphere counted less than 70% of the other hemisphere. Otherwise, the language dominance was considered bilateral.

Language MEG

The MEG signals were recorded with a 204-channel biomagnetometer (VectorView; Neuromag, Helsinki, Finland) in a magnetically shielded room. To confirm the reproducibility, we acquired two data sets for each task by repeating the MEG recording on two different days. One hundred fifty nouns consisting of three *Kana* letters were visually presented with a 300-millisecond exposure time with interstimuli intervals ranging from 2800 to 3200 milliseconds. Patients were instructed to judge whether or not the presented word was "abstract" or "concrete" based on the nature of the word and to push a button with the index or middle finger (*Kana* reading task). Each epoch consisted of a 500-millisecond prestimulus baseline and a stimulus followed by a 1500-millisecond analysis period. Epochs with a reaction time exceeding 1200 milliseconds and MEG examinations with a successful task performance less than 70% were discarded.

One hundred fifty epochs of the magnetic signals were averaged and digitally filtered between 0.1 to 30 Hz. Significant MEG deflections were visually identified based on the square root mean fields of more than 10 sensors in the frontotemporal (FT) or temporo-occipital (TO) regions. Locations and dipole moments of equivalent current dipoles were calculated every 2 milliseconds from 250 to 600 milliseconds after the stimulus onsets using the single equivalent dipole and sphere head models. Only those dipoles of which the measured and the calculated field distributions showed a correlation value of more than 0.85 and confidence volumes less than 1000 mm^3 were used. To confirm the calculated results, the same MEG time sections were analyzed using a current density map (low-resolution tomography; LORETA, Curry, Neuroscan, and Compumedics USA, El Paso, TX). The coordinates of the MEG system were transformed into anatomic 3D-MRI scans by identifying external anatomic fiduciary markers (nasion, left/right preauricular points), and estimated dipoles were superimposed onto the 3D-MRI scans.

Dipoles located in the temporal region, including the STG, MTG, SmG, and FuG, were manually counted. A patient was considered to have unilateral language dominance when hemispheric dipoles of one hemisphere counted less than 70% of the other hemisphere. Otherwise, the language dominance was considered bilateral.

Determination of Language Dominance using fMRI and MEG

On the basis of the results of language fMRI and MEG, we determined language dominance for each patient. When the semantic activation in one side of the IFG and MFG was wider than that of the other side during the language fMRI tasks, a patient was considered to have unilateral dominance for the expressive language function. When one side of the temporal region included more MEG dipoles than the other during the language MEG task, we determined that a patient had laterality of the receptive language function.

The Wada Test

All patients received injections of amobarbital (100 mg in a 10% solution, Amytal; Eli Lilly and Co., Indianapolis, IN) through a catheter placed in the internal carotid artery. Language testing was performed during the observation period of maximal amobarbital action as indicated by contralateral

brachial plegia. Patients were given the following tasks in the following order and up to four points were given, depending on the severity of the language disturbance: 0, no response; 1, meaningless utterance; 2, incorrect repetition or paraphasia; 3, self-correction; and 4, unimpaired.

The tasks were as follows:

1) Spontaneous counting. Patients were instructed to count, starting immediately before the amobarbital administration and continuously until the next task was given. If the patient could continue to count even after brachial plegia appeared, obvious speech arrest and no impairment indicate 0 and 4 points, respectively.
2) Letter reading. Patients were instructed to read aloud seven words consisting of three or four *Kana* letters. The maximum score was 28 points (seven items × four points).
3) Naming. Patients were asked to name aloud the five objects presented pictorially. The maximum score was 20 points (five items × four points).
4) Auditory comprehension. Patients were asked to carry out three simple tasks such as blinking eyes, opening the mouth, and raising the unparalyzed arm. The maximum score was 12 points (three items × four points).
5) Pointing objects. Patients were shown a picture with a set of four objects and were instructed to point to one chosen by the investigator (e.g., "Point to the cat."). The maximum score was 16 points (four items × four points).

Performance in Tasks 1 and 3 were considered to reflect the expressive language capabilities (maximum score, 24 points); performance in Tasks 2, 4, and 5 reflected receptive language functions (maximum score, 56 points).

RESULTS

Handedness and the Wada Test

Ninety-one patients (80 right-, eight left-, and three bilateral-handers) successfully underwent the Wada test. Language dominance was left, right, and bilateral hemispheres in 81, six, and four patients, respectively. The language dominance of the right-handed patients was left in 75 patients (93.8%), right in two patients (2.5%), and bilateral in three patients (including one patient with dissociated expression and receptive functions [3.8%]), respectively. For left-handed patients, four patients showed left and four showed right dominance. For both-handed patients, two showed left dominance and one bilateral (dissociated). These results were similar to those of previous reports on language dominance (3, 4).

For further analysis, we subdivided the subjects into groups with chronic epilepsy and with non-epilepsy. In the epilepsy group (n = 29), left, right, and bilateral dominance was 24 (82.8%), three (10.3%), and two (6.9%), respectively. In the non-epilepsy group (n = 62), left, right, and bilateral dominance was 57 (91.6%), four (6.4%), and one (1.6%), respectively.

fMRI with the Verb Generation Task

The verb generation task was designed to locate the expressive language area by fMRI. Among 117 patients who underwent the verb generation task, 100 patients (84.6%) completed the task and provided useful fMRI data. The results showed that the dominant hemisphere for the expressive language function was left, right, and bilateral in 90, eight, and two patients, respectively. In the epilepsy group (n = 34), left, right, and bilateral dominance was 29 (85.2%), three (8.8%), and two (8.5%), respectively. In the non-epilepsy group (n = 66), left, right, and bilateral dominance was 61 (92.4%), five (7.6%), and zero (0%), respectively. The activated regions on fMRI mainly involved the IFG and MFG, the lateral precG, AG, and the supplementary motor area (SMA) (*Figs. 1* and *2*).

In some patients, activations were observed in bilateral hemispheres. Except for two patients who showed bilateral dominance, the activations in the non-dominant hemisphere were restricted to MFG and precG and smaller in size, so the pixels did not reach a cluster significance (maximum values of Z-score, <2.2 or <10 pixels).

Compared with successful results of the Wada test, the successful rate of fMRI with the verb generation task was 90.1%. Seven patients with aphasia or dementia failed to complete the task. Three glioma patients with marked surrounding, four patients with brain ischemia and three patients with large arteriovenous malformations failed to exhibit significant activations in the frontal lobe (*Fig. 3*). These incomplete results are accounted for by the reported disadvantage of fMRI that data may be affected by the pathological changes of cerebral circulation (7, 10, 15).

fMRI with the A/C Categorization Task

The A/C categorization task was designed to locate the receptive language area by fMRI. Among 106 patients who performed the A/C categorization task, 71 (67.0%) completed the task and provided useful fMRI data. Compared with the verb generation task, the A/C categorization task more often activated wider areas in bilateral hemispheres (*Fig. 2*). Activations generally involved the bilateral frontal lobes, including the IFG, MFG, and precG, with laterality. The superior temporal regions, such as the STG and SmG, demonstrated activation spots in only 45% (n = 32) of the investigated patients, and the side predominance was not apparent in most cases. The fMRI data of the A/C categorization task were considered unsuitable to determine the receptive language areas and were not used for the final analyses.

Language MEG Profiles and Dipole Locations

The *Kana* reading task was designed to locate the receptive language area by MEG. The language MEG was performed in 117 patients, of whom 99 (85.4%) completed the task and provided useful data (*Figs. 1* and *2*). Results showed that the dominant hemisphere for the receptive language function was left, right, and bilateral in 85, 11, and three patients, respectively. In the epilepsy group (n = 31), left, right, and bilateral dominance was 26 (83.9%), three (9.7%), and two (6.5%), respectively. In the non-epilepsy group (n = 68), left, right, and bilateral dominance was 59 (86.8%), eight (11.8%), and one (1.5%), respectively.

Dipole clusters of late deflections localized mainly in the superior temporal region (STG, MTG, and SmG), and 60% of investigated patients also showed dipoles in the inferior tempo-

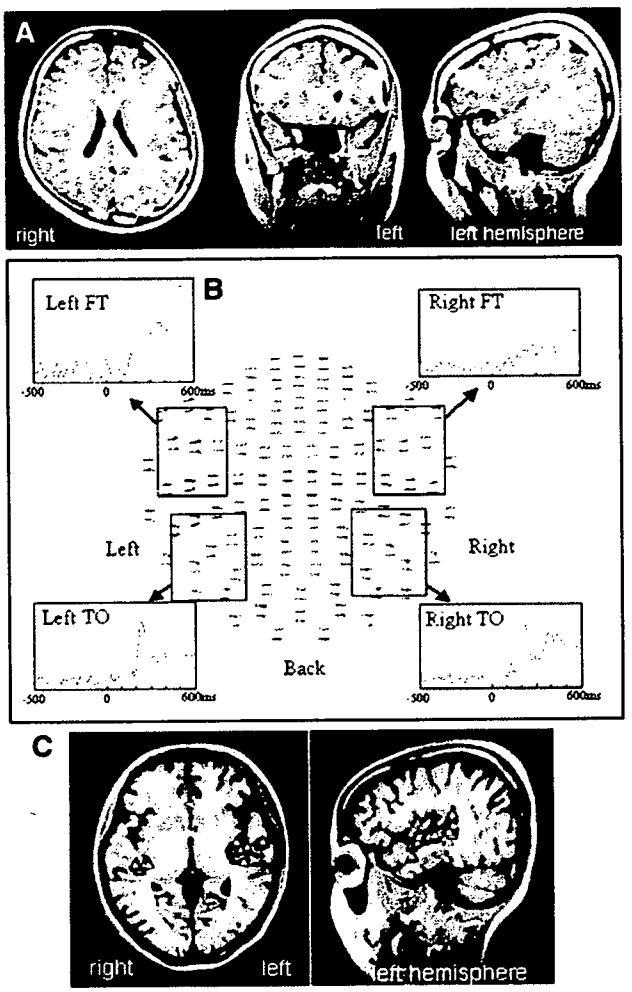

FIGURE 1. *A 24-year-old, right-handed man with epilepsy. A, fMRI with the verb generation task showing activations predominantly in the left IFG, MFG, PrecG, and parieto-occipital regions. B, square root mean field profiles of language MEG responses in the bilateral FT and TO regions. The left FT responses, peaking at 450 milliseconds, were markedly greater in amplitude than the right FT. C, source localization of the late deflections showing predominant dipole clusters (arrowheads) in the left superior temporal region. The left and right hemispheres contained 97 and 37 dipoles, respectively.*

ral region (FuG and inferior temporal gyrus). In 96 patients who showed unilateral language dominance, the total number of dipoles in the dominant versus non-dominant hemispheres was 124.1 ± 62.1 and 58 ± 30.9 (mean ± standard deviation), respectively. The ratio of the dipole number in the dominant hemisphere to the non-dominant hemisphere in each individual was 2.4 ± 1.7 (range, 1.43–14.4).

A typical result with all channels of MEG with the *Kana*-reading task is illustrated in *Figure 1*. Later deflections peaking at approximately 400 milliseconds were predominantly observed in the left FT. Bilateral TO regions demonstrated early deflections at approximately 200 milliseconds with short durations and little laterality. Estimated dipoles of the FT regions were densely accumulated in the left STG, MTG, and SmG (102 dipoles), whereas the right hemisphere showed fewer dipoles (54 dipoles) in the superior temporal region. This patient was thus determined to have receptive language dominance in the left temporal lobe.

The successful rate of language-MEG was 82.4%. Nine out of 39 epilepsy patients (23.1%) could not provide useful MEG data owing to artifacts from constant eye movements; the *Kana*-reading task was more difficult to complete than the verb generation task for patients with mental dysfunction. On the other hand, only one out of 18 AVM patients, owing to severe dyslexia, failed to provide useful MEG data, indicating that, in contrast to fMRI, MEG was not frequently affected by cerebral blood flow abnormalities (*Fig. 3*).

Combination of fMRI and MEG with Wada Test Verification

The verb generation task fMRI data depict expressive language areas well, but may be affected by cerebral blood flow abnormalities. The MEG results indicate receptive language areas well, but the task is rather complicated and may not be suited for patients with mental disorders. We sought to establish a non-invasive and reliable method to determine the laterality of language dominance by combining the advantages of these approaches. Furthermore, in terms of language functions, the results from fMRI and MEG can be integrated to locate expressive and receptive language areas and to provide reliable evidence whether or not there is dissociation. To verify the reliability of our method, 97 patients also underwent the Wada test.

Useful data from the method co-utilizing fMRI and MEG could be obtained from 87 out of 91 patients (95.6%). Remarkably, regarding language dominance, the results from the combination method matched the results of the Wada test in all 87 patients. Worth noting is that two patients (one with left temporal lobe epilepsy and the other with right insular astrocytoma) showed dissociated language areas using the combined method. The expressive language area was depicted in the left frontal lobe by fMRI, but the receptive language area was demonstrated in the right temporal lobe by MEG (*Fig. 4*). The Wada test results confirmed that both patients have language functions dissociated in the bilateral hemispheres. Among the 91 patients who underwent the Wada test, these were the only two patients in whom the Wada test detected dissociation of language functions.

In 12 epilepsy patients, the expressive and/or receptive language areas were electrophysiologically investigated via a subdural electrode implantation and the results were compared with those determined via the combined fMRI plus MEG method (*Fig. 5*). Out of eight patients who underwent cortical mapping for the expressive language area, all showed a speech arrest by electrical stimulation to the IFG and four to the MFG. All of the physiologically determined locations were confined within the areas depicted by the combined method. Out of six patients who received electrical stimuli to the temporal lobe,

four showed responses interpretable as impaired speech comprehension. In all such cases, the electrophysiologically determined location matched the area depicted by the combined method, although MEG-depicted receptive language areas covered relatively broad areas of the temporal lobe. The regions determined by the combined method were always broader, but had the border within the adjacent gyri of those determined by electrophysiological mapping.

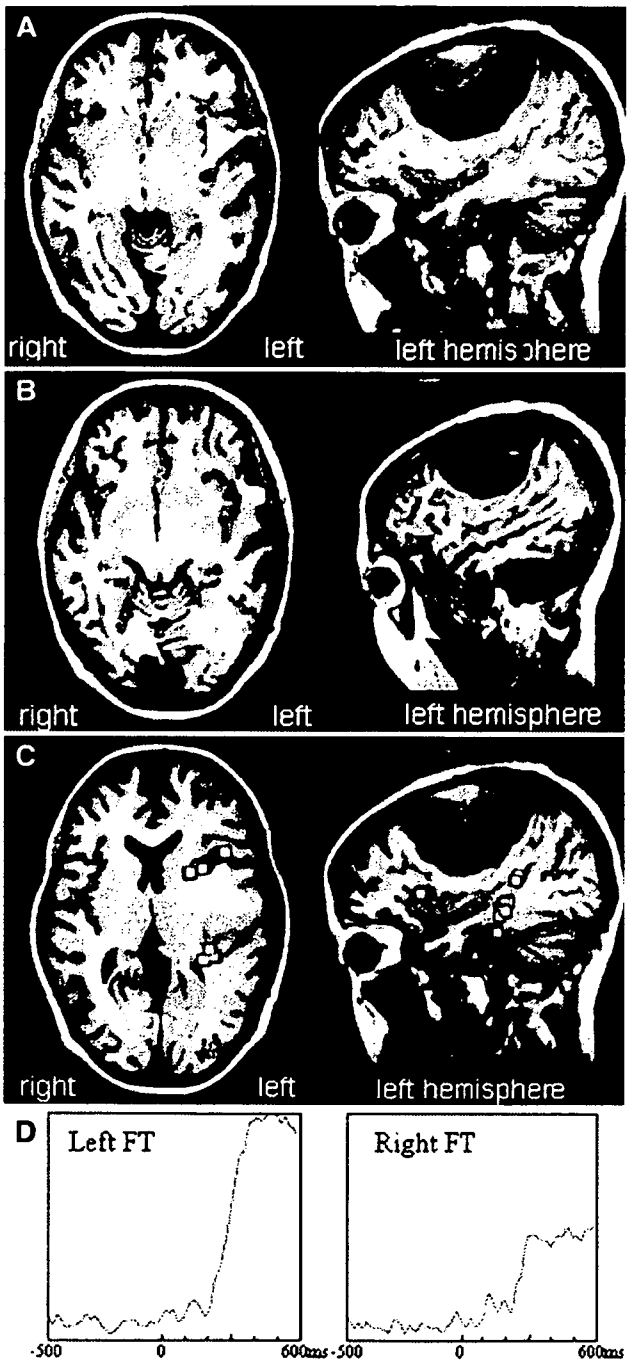

ILLUSTRATIVE CASES

Patient 1

A 16-year-old, right-handed female patient had experienced transient numbness in her left upper extremity with a 2-month history. T1-weighted MRI scans demonstrated an extra-axial cystic lesion in the left frontal region. Although the lesion markedly compressed the frontal lobe, she had no impairment of language and motor functions. fMRI with the verb generation task demonstrated obvious activation in the left IFG and MFG shifted inferiorly by the lesion (*Fig. 2A*). The A/C categorization task activated a small area of the left IFG, but mainly the bilateral occipital lobes. Concerning MEG with the *Kana* reading task, RMS of the left FT was much higher than that of the right, and numbers of semantic dipoles were 117 and 30 in left and right hemispheres, respectively. The main dipole clusters were located in the left IFG and STG. The tumor was totally removed and histopathological diagnosis was meningioma.

Patient 2

A 24-year-old, right-handed male patient had a large AVM in the left frontal lobe. fMRI detected little activation in the IFG or MFG, although a part of the left angular gyrus was activated by the verb generation task (*Fig. 3A*). MEG, however, disclosed numerous dipole accumulations in the left superior temporal region. In the MEG examination, the left and right hemispheres contained 130 and 45 dipoles, respectively, suggesting left language dominance (*Fig. 3B*). Auditory comprehension and letter-reading were suppressed by administration of amobarbital into the left carotid artery, although motor language function was preserved. These findings suggested that the steal effect caused by the AVM partly interfered with functional brain mapping of fMRI and the Wada test. In this case, MEG was helpful to decide language dominance (*Fig. 3*).

Patient 3

A 32-year-old, right-handed man experienced amnesia for several minutes. T1-weighted MRI scans and brain computed tomographic scans disclosed a hypointense and hypodense mass in the right insular cortex involving the surrounding white matter. Computed tomographic scans performed 6 years earlier, however, revealed no abnormality. These findings suggested that a low-grade astrocytoma might

FIGURE 2. *A 16-year-old, right-handed female patient with a large meningioma in the left frontal region. The patient had no impairment of language or motor functions.* A, *fMRI with the verb generation task showed activations mainly in the left IFG and MFG that shifted inferiorly by the tumor.* B, *fMRI with the abstract/concrete categorization task demonstrated activations in the bilateral occipital regions in addition to small active spots in the left IFG.* C, *square root mean field profiles of language-MEG responses demonstrated that the left FT responses, peaking at 400 milliseconds, were markedly larger in amplitude than the right FT.* D, *source localization of the late deflections showed predominant dipole clusters in the left posterior temporal region. The left and right hemispheres contained 117 and 30 dipoles, respectively. The combined fMRI plus MEG method indicated left language dominance, which was confirmed by Wada test.*

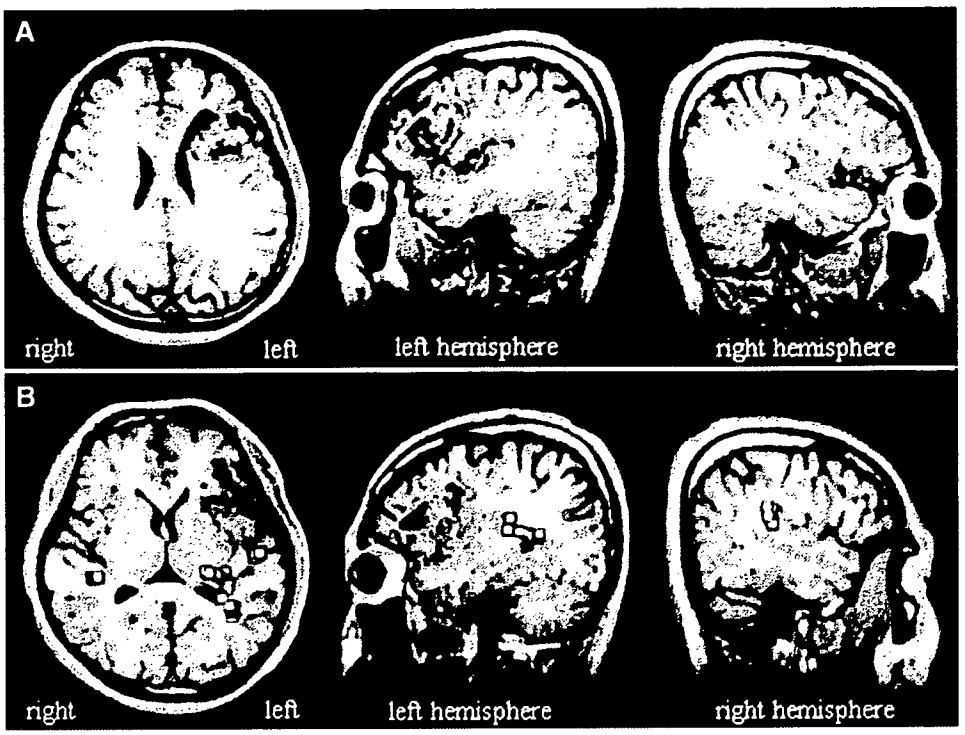

FIGURE 3. *A 24-year-old, right-handed man with a large AVM in the left frontal lobe.* A, *fMRI with the verb generation task showed little activation in the left frontal lobe where the AVM was located.* B, *source localization of the late FT and TO deflections on MEG showed predominant dipole clusters in the left posterior STG. The left and right hemispheres contained 123 and 51 dipoles, respectively.*

have slowly developed during the past 6 years. In the results of the verb generation task, the left hemisphere had obvious activations in the IFG, MFG, precG, and the angular gyrus, indicating that this patient had left dominance of motor-language functions (*Fig. 4A*). In contrast, estimated dipoles of the FT responses were concentrated in the posterior part of the right STG and MTG (138 dipoles) and another dipole cluster (64 dipoles) of the TO region was localized in the right FuG. The total dipole number of the left hemisphere (48 dipoles) did not reach even a quarter of that of the right hemisphere, suggesting right-sided dominance of temporal language functions (*Fig. 4*).

During the Wada test, he stopped counting (0 out of 4 points; 0%) and failed to name objects (6 out of 20 points; 30%) after left intracarotid injection, whereas letter-reading (21 out of 28 points; 75%), auditory comprehension (12 out of 12 points, 100%), and pointing objects tasks (16 out of 16 points; 100%) were well preserved. In contrast, after right intracarotid injection, letter reading (13 out of 28 points; 45%), auditory comprehension (3 out of 12 point; 25%), and pointing objects (4 out of 16 points; 25%) tasks were markedly suppressed, although he continued to count correctly without speech blockade (4 out of 4 points; 100%) and could perform naming (17 out of 20 points; 85%). These findings suggested that language functions were distributed separately over the bilateral hemispheres, and the expressive and receptive language functions were dissociated in the left frontal and right temporal lobes, respectively. A striking fact was that the combination of fMRI and MEG predicted the special profiles of language functions noninvasively.

DISCUSSION

We demonstrated that our method using both fMRI with the verb generation task and MEG with the *Kana* reading task is highly reliable in determining the language dominance in patients with brain lesions. The accuracy of the dominance laterality was confirmed by a 100% match with the results from the Wada test. fMRI and MEG compensated each other's disadvantages. The tasks of fMRI were rather simple and could be accomplished even by patients with mental dysfunctions, whereas MEG results were seldom affected by cerebral blood flow abnormalities. Reliable data on language functions were also obtained by combining the advantageous features of fMRI and MEG. fMRI with the verb generation task well depicted the expressive language area as activations in the frontal lobe, most commonly in the IFG. MEG, on the other hand, showed dipole clusters predominantly in the superior temporal regions representing the receptive language area. In the epilepsy group, left and bilateral dominance were approximately 85% and more than 6%, respectively, whereas, in the non-epilepsy group, left and bilateral dominance were more than 90% and less than 2%, respectively. The combined method, including the Wada test, fMRI, and MEG, clearly demonstrated bilateral dominance is more often observed in the epilepsy group than in the non-epilepsy group.

In our study, two out of 87 patients analyzed (2.3%) were found to have dissociation of the expressive and receptive language functions by co-utilization of fMRI and MEG, verified by the Wada test, which best described the usefulness of our method in identifying the areas of the two language functions separately. In both cases, neither modality alone demonstrated the dissociation. Although several cases have been reported that dissociated language functions were found by fMRI, none of those was proven by the Wada test (2, 8, 21, 23). Our results show that neither fMRI nor MEG alone is sufficient to accurately locate the expressive and receptive language areas, and the combined use is the key to obtaining high reliability.

The results from electrophysiological investigation via a subdural electrode implantation in 12 patients further confirmed the accuracy of the present method. Pouratian et al. (22) reported that the sensitivity and specificity of language-fMRI

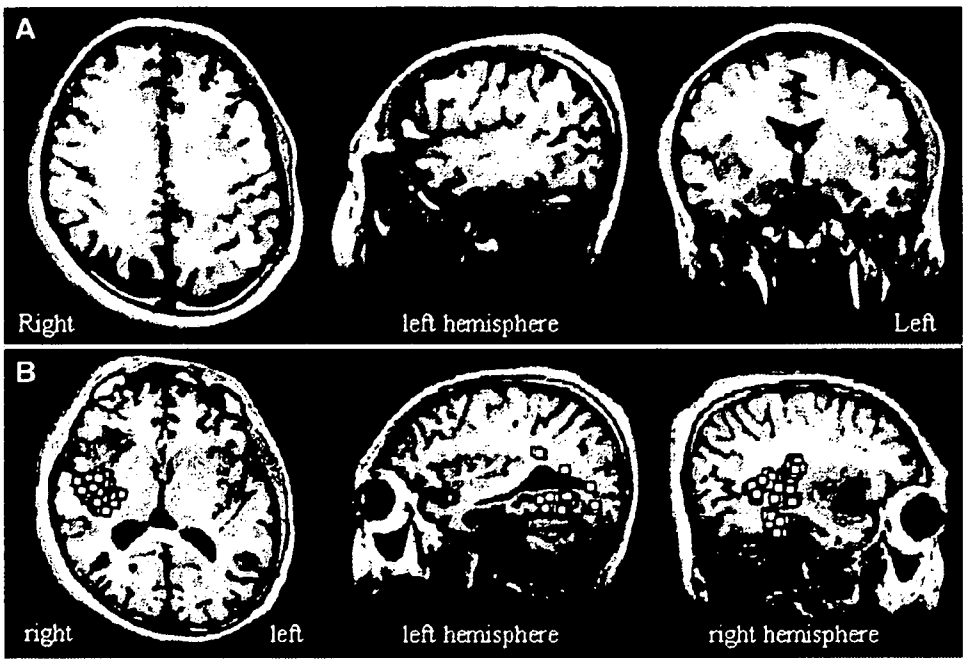

FIGURE 4. *A 32-year-old, right-handed man with astrocytoma in the right insular cortex and the surrounding white matter. A, fMRI with the verb generation task showed main activations in the IFG, MFG, precG, and AG, indicating left dominance of the expressive language function. B, in contrast to the fMRI results, source localization of the late FT deflections on MEG showed predominant dipole clusters in the right temporal lobe. The left and right hemispheres contained 48 and 202 dipoles, respectively. The combined fMRI plus MEG method thus indicated dissociated frontal motor and temporal receptive language functions. This result was confirmed by the Wada test. The patient showed impaired counting and object naming after amobarbitol injection into the left carotid artery. In contrast, letter reading, auditory comprehension and object pointing tasks were markedly suppressed, without counting impairment and speech blockade, after amobarbitol injection into the right carotid artery.*

were dependent on the task, lobe, and matching criterion. The sensitivity and specificity of fMRI activations during expressive linguistic tasks in the frontal lobe were found to be up to 100 and 66.7%, respectively, in the frontal lobe. FitzGerald et al. (6) reported that sensitivity and specificity for all multiple language tasks ranged from 81 to 53% (6). On the other hand, several groups have reported that the language map obtained from fMRI poorly matched the intraoperative electrical stimulation mapping (6, 25). In our study of language-fMRI, every electrical stimuli to the IFG, where the fMRI-activation was observed, caused speech arrest. However, the stimulation to MFG caused language-related symptoms in only half of patients. Although the sensitivity of fMRI might be high, there are still several issues of individual variability of fMRI activation and semantic tasks. The discrepancy can be partly accounted for by the fundamental differences in methodology such that the electrical stimulation directly blocks the specific language functions, whereas fMRI picks up all activated areas involved in the language tasks. Therefore, fMRI-based mapping largely depends on the design of the performing task. We tested two different tasks for fMRI and found the verb generation task better suited for language mapping than the A/C categorization task. The significance of activations depicted on fMRI is still under debate. Language-fMRI activations may be related to various semantic components of the task, including the will to retrieve verbal materials and the memory related to articulations. Despite that the A/C categorization task was designed to detect the receptive language area, activations in the temporoparietal region was less frequently observed than in the frontal region. Neural activities in the temporoparietal area are considered relatively scarce (25), and the discrepant activities of the frontal and temporoparietal regions may be owing to physiological variations of brain regions. Alternatively, the frontal and temporal lobes may have different oscillations (brain rhythms) of brain activity in response to verbal tasks, which are reflected in changes in neuronal currents and cerebral blood flow.

Our study demonstrated that dominance of the receptive language function could be accurately determined by MEG. For that purpose, we originally designed the task of three-letter word reading and silent categorization and used the dipoles calculated from late deflections to process the MEG results. It has been reported that cortical evoked potentials recorded by subdural electrodes showed responses at approximately 200 (early) and 400 (late) milliseconds in the left temporal lobe cortex after letter presentation (1, 17). The late potentials have been noted especially in tasks involving decisions based on visually presented words (13, 14). In this study, the sources of late responses (250–600 ms) were located mostly in the posterior temporal region, and the laterality of dipole clusters accurately reflected the receptive language dominance. It has been reported that dipoles in the superior temporal region showed an excellent agreement with an intraoperative electrical mapping (27). We also included dipoles in the FuG for language dominance determination based on our experience with a case in which an injury of FuG resulted in pure dyslexia (12). These contrivances in our method may have led to improvement in accuracy on language dominance determination over previous reports (20). Basic technical issues of the MEG investigation still remain. Eye movement artifacts were strong enough to distort the baseline of the MEG data. In our study,

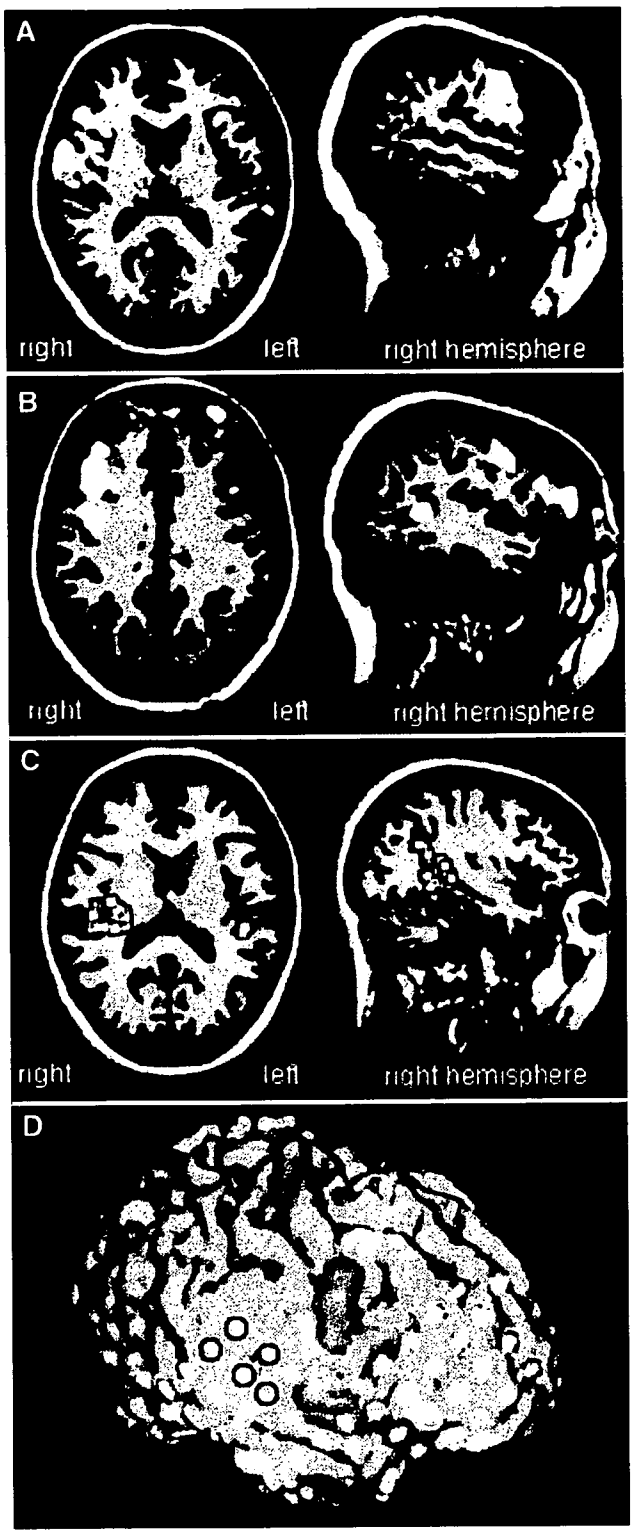

we asked patients to keep gazing at the center of the screen during the semantic decision without blinking. As a result, artifacts were observed at later than 600 milliseconds after letter presentation and usually did not affect the early and late semantic responses. It is, however, important to prevent artifacts by monitoring eye movements and using rejection thresholds.

In conclusion, by co-utilizing fMRI and MEG, we established a method to determine language dominance with a high reliability. The fMRI activations with the verb generation task identified the expressive language area, whereas the language MEG dipoles located the receptive language areas. Our institution is now routinely using the combined technique to identify the language dominance. If it does not produce data on cerebral dominance, we additionally perform the Wada test before surgery. This non-invasive and repeatable method may be an effective alternative to the Wada test and may be useful in the management of patients with brain lesions.

Disclosure

This work was supported in part by the Japan Epilepsy Research Foundation, Takeda Promotion of Science Foundation, a grant-in-aid No.17591502 for scientific research from MEXT, a Research Grant of the Princess Takamatsu Cancer Research Fund, Terumo Promotion of Science Foundation, Brain Science foundation, and Grant-in-Aid No. 18020010 for Scientific Research on Priority Areas Integrative Brain Research from MEXT.

REFERENCES

1. Allison T, McCarthy G, Nobre A, Puce A, Belger A: Human extrastriate visual cortex and the perception of faces, words, numbers, and colors. **Cereb Cortex** 4:544–554, 1994.
2. Baciu MV, Watson JM, McDermott KB, Wetzel RD, Attarian H, Moran CJ, Ojemann JG: Functional MRI reveals an interhemispheric dissociation of frontal and temporal language regions in a patient with focal epilepsy. **Epilepsy Behav** 4:776–780, 2003.
3. Branch C, Milner B, Rasmussen T: Intracarotid sodium amytal for the lateralization of cerebral speech dominance: Observations in 123 patients. **J Neurosurg** 21:399–405, 1964.
4. Brazdil M, Zakopcan J, Kuba R, Fanfrdlova Z, Rektor I: Atypical hemispheric language dominance in left temporal lobe epilepsy as a result of the reorganization of language functions. **Epilepsy Behav** 4:414–419, 2003.
5. Chen HM, Varshney PK: Mutual information-based CT-MR brain image registration using generalized partial volume joint histogram estimation. **IEEE Trans Med Imaging** 22:1111–1119, 2003.

FIGURE 5. *A 40-year-old, left-handed woman with epilepsy.* A, *fMRI with the verb generation task showed activations predominantly in the right IFG and MFG.* B, *fMRI with the A/C categorization task demonstrated activations in the right MFG and the posterior STG.* C, *source localization of the late deflections on MEG showed predominant dipole clusters* (white squares) *in the right posterior temporal region. The left and right hemispheres showed 44 and 144 dipoles, respectively.* D, *three-dimensionally reconstructed MRI scans fused with activation of the verb generation-fMRI* (orange) *and dipoles of language-MEG* (blue). *After implantation of subdural electrodes* (gold), *cortical mapping was performed with 50Hz bipolar electrical stimulation. Stimulation with intensity of 7mA to the right IFG caused speech arrest* (white circles), *whereas stimulation to the posterior STG caused impairment of auditory comprehension and reading capability* (black circles).

6. FitzGerald DB, Cosgrove GR, Ronner S, Jiang H, Buchbinder BR, Belliveau JW, Rosen BR, Benson RR: Location of language in the cortex: A comparison between functional MR imaging and electrocortical stimulation. **AJNR Am J Neuroradiol** 18:1529–1539, 1997.
7. Holodny AI, Schulder M, Liu WC, Maldjian JA, Kalnin AJ: Decreased BOLD functional MR activation of the motor and sensory cortices adjacent to a glioblastoma multiforme: Implications for image-guided neurosurgery. **AJNR Am J Neuroradiol** 20:609–612, 1999.
8. Holodny AI, Schulder M, Ybasco A, Liu WC: Translocation of Broca's area to the contralateral hemisphere as the result of the growth of a left inferior frontal glioma. **J Comput Assist Tomogr** 26:941–943, 2002.
9. Janszky J, Ollech I, Jokeit H, Kontopoulou K, Mertens M, Pohlmann-Eden B, Ebner A, Woermann FG: Epileptic activity influences the lateralization of mesiotemporal fMRI activity. **Neurology** 63:1813–1817, 2004.
10. Kamada K, Houkin K, Iwasaki Y, Takeuchi F, Kuriki S, Mitsumori K, Sawamura Y: Rapid identification of the primary motor area by using magnetic resonance axonography. **J Neurosurg** 97:558–567, 2002.
11. Kamada K, Kober H, Saguer M, Moller M, Kaltenhauser M, Vieth J: Responses to silent Kanji reading of the native Japanese and German in task subtraction magnetoencephalography. **Brain Res Cogn Brain Res** 7:89–98, 1998.
12. Kamada K, Sawamura Y, Takeuchi F, Houkin K, Kawaguchi H, Iwasaki Y, Kuriki S: Gradual recovery from dyslexia and related serial magnetoencephalographic changes in the lexicosemantic centers after resection of a mesial temporal astrocytoma. Case report. **J Neurosurg** 100:1101–1106, 2004.
13. Kutas M, Hillyard SA: Reading senseless sentences: Brain potentials reflect semantic incongruity. **Science** 207:203–205, 1980.
14. Kutas M, Hillyard SA: Brain potentials during reading reflect word expectancy and semantic association. **Nature** 307:161–163, 1984.
15. Lehericy S, Biondi A, Sourour N, Vlaicu M, du Montcel ST, Cohen L, Vivas E, Capelle L, Faillot T, Casasco A, Le Bihan D, Marsault C: Arteriovenous brain malformations: Is functional MR imaging reliable for studying language reorganization in patients? Initial observations. **Radiology** 223:672–682, 2002.
16. Lehericy S, Cohen L, Bazin B, Samson S, Giacomini E, Rougetet R, Hertz-Pannier L, Le Bihan D, Marsault C, Baulac M: Functional MR evaluation of temporal and frontal language dominance compared with the Wada test. **Neurology** 54:1625–1633, 2000.
17. Nobre AC, Allison T, McCarthy G: Word recognition in the human inferior temporal lobe. **Nature** 372:260–263, 1994.
18. Oldfield RC: The assessment and analysis of handedness: The Edinburgh inventory. **Neuropsychologia** 9:97–113, 1971.
19. Papanicolaou AC, Simos PG, Breier JI, Zouridakis G, Willmore LJ, Wheless JW, Constantinou JE, Maggio WW, Gormley WB: Magnetoencephalographic mapping of the language-specific cortex. **J Neurosurg** 90:85–93, 1999.
20. Papanicolaou AC, Simos PG, Castillo EM, Breier JI, Sarkari S, Pataraia E, Billingsley RL, Buchanan S, Wheless J, Maggio V, Maggio WW: Magnetocephalography: A noninvasive alternative to the Wada procedure. **J Neurosurg** 100:867–876, 2004.
21. Petrovich NM, Holodny AI, Brennan CW, Gutin PH: Isolated translocation of Wernicke's area to the right hemisphere in a 62-year-man with a temporoparietal glioma. **AJNR Am J Neuroradiol** 25:130–133, 2004.
22. Pouratian N, Bookheimer SY, Rex DE, Martin NA, Toga AW: Utility of preoperative functional magnetic resonance imaging for identifying language cortices in patients with vascular malformations. **Neurosurg Focus** 13:E4, 2002.
23. Ries ML, Boop FA, Griebel ML, Zou P, Phillips NS, Johnson SC, Williams JP, Helton KJ, Ogg RJ: Functional MRI and Wada determination of language lateralization: A case of crossed dominance. **Epilepsia** 45:85–89, 2004.
24. Roux FE, Boulanouar K, Lotterie JA, Mejdoubi M, LeSage JP, Berry I: Language functional magnetic resonance imaging in preoperative assessment of language areas: Correlation with direct cortical stimulation. **Neurosurgery** 52:1335-1345, 2003.
25. Rutten GJ, Ramsey NF, van Rijen PC, Noordmans HJ, van Veelen CW: Development of a functional magnetic resonance imaging protocol for intraoperative localization of critical temporoparietal language areas. **Ann Neurol** 51:350–360, 2002.
26. Rutten GJ, Ramsey NF, van Rijen PC, van Veelen CW: Reproducibility of fMRI-determined language lateralization in individual subjects. **Brain Lang** 80:421–437, 2002.
27. Simos PG, Papanicolaou AC, Breier JI, Wheless JW, Constantinou JE, Gormley WB, Maggio WW: Localization of language-specific cortex by using magnetic source imaging and electrical stimulation mapping. **J Neurosurg** 91:787–796, 1999.
28. Woermann FG, Jokeit H, Luerding R, Freitag H, Schulz R, Guertler S, Okujava M, Wolf P, Tuxhorn I, Ebner A: Language lateralization by Wada test and fMRI in 100 patients with epilepsy. **Neurology** 61:699–701, 2003.
29. Yetkin FZ, Mueller WM, Morris GL, McAuliffe TL, Ulmer JL, Cox RW, Daniels DL, Haughton VM: Functional MR activation correlated with intraoperative cortical mapping. **AJNR Am J Neuroradiol** 18:1311–1315, 1997.

COMMENTS

This is an interesting article evaluating the complementary features of functional magnetic resonance imaging (fMRI) and magnetoencephalography (MEG) to assess language lateralization in 87 patients. Whereas any test of language lateralization is suspect if 100% correlation is found, the authors have carefully described their techniques and the analysis of results. It is quite apparent that fMRI with verb generation tasks is best at activating anterior language areas, whereas abstract versus concrete naming tasks can be less robust. This is a good article and a large experience worthy of publication.

G. Rees Cosgrove
Burlington, Massachusetts

The authors have applied fMRI and MEG techniques to localize speech function in a large number of patients with different brain lesions. They were able to supplement the two noninvasive tests with the Wada test in 80% of the patients. They were able to obtain useful data with the co-utilization of fMRI and MEG in 95.6% of the patients and found a somewhat surprisingly good match with the results of the Wada test in 100% of those. In the results section, the authors discuss a few differences to the localization of language areas by electrophysiological means. They point out the fact that atypical language dominance or bilateral language representation is more frequent in patients with chronic epilepsy than in those without epilepsy. This is an important fact not known to many neurosurgeons who are not ordinarily involved with epilepsy cases. The results of this study make it more likely that, in the future, the invasive Wada test procedure might be abolished in those institutions at which MEG is available. This constitutes a notable limitation of this noninvasive technique. If fMRI is used alone, the success rate for obtaining useful data is 84.6% for word generation tasks and only 67% for the abstract/concrete categorization task. This is quite an interesting study and the results are very promising; however, the limitations are not economical. A number of patients cannot complete all the tasks necessary for fMRI study, and MEG studies can be disturbed by eye movement artifacts. We look forward to other reports confirming these promising results.

Johannes Schramm
Bonn, Germany

The authors present some very interesting data in the realm of functional imaging to determine cerebral dominance for language. Currently, the standard modality for determining cerebral dominance is the venerable Wada test. In this study, the authors use both MEG and fMRI to determine language dominance based on activation in the inferior frontal gyrus and middle frontal gyrus using fMRI and dipole moments reflecting or indicating receptive language fields in the temporal lobe. As expected, they had some difficulty with the fMRI data owing to the underlying deficit in the patient, which suggests that fMRI is not always as good as one might expect in terms of determin-

ing cerebral dominance using a verb generation silent language task. We know that fMRI is not a good choice for defining receptive language fields that correspond to intraoperative stimulation mapping. However, when fMRI was used together with MEG, the authors were able to demonstrate 100% concordance with data from the Wada test. Thus, this is a very important study indicating that, in the near future, it may be possible to bypass the Wada test with these two powerful functional imaging modalities. That being said, not every institution is going to be able to obtain both of these functional tests. Therefore, it is unlikely that this strategy is going to replace Wada tests completely. Yet, this is a very important line of investigation and a novel observation that points out the frailties of functional imaging for cerebral dominance localization and the potential power when the different functional tests are combined.

Mitchel S. Berger
San Francisco, California

Portrait of James Figg (1695–1734), by William Hogarth, (1697–1764). Acknowledged in Britain as the "Father of Boxing," Figg popularized the sport with teaching and exhibitions and, following victories over all the other British contenders, declared himself "heavyweight champion of England" in 1719.

Oncogene (2007) 26, 5577–5586

www.nature.com/onc

ORIGINAL ARTICLE

Neuropilin-1 promotes human glioma progression through potentiating the activity of the HGF/SF autocrine pathway

B Hu[1], P Guo[1,2], I Bar-Joseph[1,2], Y Imanishi[1,2], MJ Jarzynka[1,2], O Bogler[3], T Mikkelsen[4], T Hirose[5], R Nishikawa[6] and SY Cheng[1,2]

[1]University of Pittsburgh Cancer Institute & Department of Pathology, Pittsburgh, PA, USA; [2]Department of Pathology, Research Pavilion at Hillman Cancer Center, Pittsburgh, PA, USA; [3]Department of Neurosurgery & Brain Tumor Center, MD Anderson Cancer Center, University of Texas, Houston, TX, USA; [4]Department of Neurosurgery, Hermelin Brain Tumor Center, Henry Ford Hospital, Detroit, MI, USA; [5]Department of Pathology, Saitama Medical University, Saitama, Japan and [6]Department of Neurosurgery, Saitama Medical University, Saitama, Japan

Neuropilin-1 (NRP1) functions as a coreceptor through interaction with plexin A1 or vascular endothelial growth factor (VEGF) receptor during neuronal development and angiogenesis. NRP1 potentiates the signaling pathways stimulated by semaphorin 3A and VEGF-A in neuronal and endothelial cells, respectively. In this study, we investigate the role of tumor cell-expressed NRP1 in glioma progression. Analyses of human glioma specimens (WHO grade I–IV tumors) revealed a significant correlation of NRP1 expression with glioma progression. In tumor xenografts, overexpression of NRP1 by U87MG gliomas strongly promoted tumor growth and angiogenesis. Overexpression of NRP1 by U87MG cells stimulated cell survival through the enhancement of autocrine hepatocyte growth factor/scatter factor (HGF/SF)/c-Met signaling. NRP1 not only potentiated the activity of endogenous HGF/SF on glioma cell survival but also enhanced HGF/SF-promoted cell proliferation. Inhibition of HGF/SF, c-Met and NRP1 abrogated NRP1-potentiated autocrine HGF/SF stimulation. Furthermore, increased phosphorylation of c-Met correlated with glioma progression in human glioma biopsies in which NRP1 is upregulated and in U87MG NRP1-overexpressing tumors. Together, these data suggest that tumor cell-expressed NRP1 promotes glioma progression through potentiating the activity of the HGF/SF autocrine c-Met signaling pathway, in addition to enhancing angiogenesis, suggesting a novel mechanism of NRP1 in promoting human glioma progression.
Oncogene (2007) **26**, 5577–5586; doi:10.1038/sj.onc.1210348; published online 19 March 2007

Keywords: neuropilin-1; HGF/SF; c-Met; glioma

Correspondence: Dr S-Y Cheng, University of Pittsburgh Cancer Institute & Department of Pathology, Suite 2.26, 5117 Centre Avenue; Pittsburgh, PA 15213-1863, USA or Dr B Hu, University of Pittsburgh Cancer Institute & Department of Medicine, Suite 2.26, 5117 Centre Avenue; Pittsburgh, PA 15213-1863, USA.
E-mail: chengs@upmc.edu or hub@upmc.edu
Received 18 September 2006; revised 18 December 2006; accepted 6 January 2007; published online 19 March 2007

Introduction

Neuropilin-1 (NRP1) is a type I cell surface co-receptor that plays important roles in the development of the nervous system and angiogenesis (Bagri and Tessier-Lavigne, 2002). During neuronal development, NRP1-mediated signal transduction requires the formation of a functional semaphorin (Sema) 3A-NRP1-plexin A1 complex, which inhibits axonal guidance signals to the projecting neurons (Bagri and Tessier-Lavigne, 2002). In endothelial cells, NRP1 enhances the interaction of heparin-binding vascular endothelial growth factor $(VEGF)_{165}$ with its receptors (VEGFRs) and modulates VEGF-stimulated angiogenesis. Elevated expression of NRP1 was also found in tumor cells in various types of human cancers (Klagsbrun *et al.*, 2002). Overexpression of NRP1 in prostate and colon cancer cells enhances angiogenesis and tumor growth in animals (Miao *et al.*, 2000; Parikh *et al.*, 2004), whereas expression of an antagonist of NRP1 inhibited vessel growth and tumor expansion (Gagnon *et al.*, 2000).

Hepatocyte growth factor/scatter factor (HGF/SF) modulates various cellular functions such as proliferation, migration and morphogenesis through its cognate surface receptor c-Met (Gao and Vande Woude, 2005). Activation of the HGF/SF/c-Met signaling pathway correlates with the malignancy of human gliomas (Abounader and Laterra, 2005). Overexpression of HGF/SF in glioma cells resulted in enhanced tumorigenicity and growth *in vivo* (Laterra *et al.*, 1997). Inhibition of endogenous HGF/SF and c-Met in human cancer cells, including gliomas, reversed their malignant phenotype (Abounader *et al.*, 2002). Additionally, the activation of signaling molecules such as extracellular signal-regulated kinase (ERK) and Bcl-2 antagonist of cell death (Bad) is involved in the HGF/SF/c-Met pathway in cancer cells (Abounader and Laterra, 2005). NRP1 was recently demonstrated to interact directly with a subset of heparin-binding growth factors, such as fibroblast growth factor-2 (FGF-2), FGF-4 and HGF/SF and potentiates FGF-2 stimulation of endothelial cells (West *et al.*, 2005), suggesting that NRP1 expression in glioma cells may augment

HGF/SF/c-Met stimulation of tumor progression through an autocrine loop.

In this study, we investigated the roles of tumor cell-expressed NRP1 in human glioma progression. We show that upregulated NRP1 is primarily expressed in tumor cells, and NRP1 expression correlates with tumor progression in clinical glioma specimens. We demonstrate that NRP1 expression promotes glioma growth and survival *in vitro* and *in vivo* through an autocrine HGF/SF/c-Met signaling pathway involving activation of c-Met, ERK and Bad, thus suggesting a novel mechanism of NRP1 expression in promoting cancer cell survival and proliferation.

Results

Upregulation of NRP1 is correlated with the malignancy of human astrocytic tumors

To determine the association of NRP1 expression with glioma progression, we performed immunohistochemistry (IHC) analyses on a total of 92 human glioma specimens and four normal human brain biopsies using three well-characterized anti-NRP1 antibodies (Ding *et al.*, 2000) and isotype matched IgGs as negative controls that all showed no staining (see the insets in Figure 1A). As shown in Figure 1Aa, in all four normal brain tissues analysed, weak immunoactivity for the anti-NRP1 antibody was detected in neurons (red arrow) or cells within a blood vessel (arrowhead). In four pilocytic astrocytoma specimens (P.A., WHO grade I), NRP1 was weakly stained in a few tumor cells (Figure 1Ab, arrows) and vessels (panel b, arrowhead). In 24 WHO grade II gliomas, NRP1 protein was detected in tumor cells (panel c, arrows) and vessels (panel c, arrowhead). In 21 WHO grade III glioma biopsies, a greater intensity of NRP1 staining was detected in tumor cells (Figure 1Ad, arrows). In 43 WHO grade IV glioblastoma multiforme (GBM) specimens, high expression of NRP1 was found in tumor cells (Figure 1Ae, arrows). In general, no increase in staining for NRP1 protein was found in hypoxic/pseudopalisading regions, but heterogeneous staining for NRP1 expression was seen within the gliomas. As summarized in Figure 1B and Supplementary Table S1 (Supplementary Material), statistical analyses of our IHC data revealed a significant correlation between NRP1 expression and human glioma progression. There was a significant difference in IHC staining for NRP1 among the three groups as well as a correlation between NRP1 expression and the malignancy of human glioma (Figure 1B).

Overexpression of NRP1 in U87MG xenografts promotes tumor growth and angiogenesis in vivo

To further investigate whether upregulation of NRP1 by glioma cells promotes tumor progression, we first examined expression of NRP1 in human glioma cell lines by immunoblot (IB) analyses. As shown in Figure 2a, NRP1 protein was detected at various levels in all glioma cell lines examined. As U87MG cells express NRP1 at a relatively low level and are highly tumorigenic in mice (Hu *et al.*, 2003), we utilized this cell line to stably overexpress NRP1. Among various U87MG cell clones that stably express NRP1, we chose two cell clones, U87MG/NRP1-no. 1 and U87MG/NRP1-no. 8, that expressed exogenous NRP1 at medium (NRP1-no. 1) or high levels (NRP1-no. 8) compared with U87MG (Figure 2b) or LacZ (see below) cells for further studies. Next, we separately implanted U87MG and NRP1 cells into the flank or the brain of nude mice. On the 26th day post-implantation, inoculation of NRP1 cells into the flank resulted in formation of tumors with an average volume of $1205 \pm 307\,mm^3$, whereas mice that received U87MG or LacZ cells (Guo *et al.*, 2001) developed tumors with similar volumes in 45 days (Figure 3A). In the brain, mice receiving NRP1 cells developed tumors with a volume of $34 \pm 6.8\,mm^3$ in 25 ± 3 days ($n = 17$) (Figure 3Bc, d and 3C), whereas mice inoculated with U87MG or LacZ cells developed tumors of $15 \pm 4.5\,mm^3$ in the same period of time ($n = 15$) (Figure 3Ba, b and 3C). Afterwards, we stained the brain tumor tissue using anti-CD31 (Figure 3Bb and d) and anti-bromodeoxyuridine (BrdUrd) plus anti-von Willebrand factor (vWF) antibodies (Figure 3E). We found that NRP1 intracranial tumors had a 2.5-fold increase in vessel density (Figure 3D) and a 2.6-fold increase in BrdUrd incorporation in the tumor cells when compared with U87MG tumors (Figure 3F).

NRP1 promotes U87MG cell growth through enhancing autocrine HGF/SF/c-Met signaling

Our results show that overexpression of NRP1 by glioma cells enhances tumor cell proliferation *in vivo*, which could possibly be due to NPR1-modulated autocrine intracellular signaling stimulation in glioma cells or caused indirectly by an increase in angiogenesis. To distinguish these possibilities, we performed a trypan blue vital dye exclusion assay. NRP1 overexpression did not significantly affect NRP1 cell growth compared with U87MG or LacZ cells when cultured in medium containing 10% fetal bovine serum (FBS) (data not shown). However, as shown in Figure 4A, in the absence of serum, NRP1 cells showed a 1.8-fold increase in cell survival, whereas U87MG or LacZ cells demonstrated a slight decrease of cell survival in a 4-day culture, suggesting that autocrine signaling through NRP1 promotes cell survival in these glioma cells.

A recent study demonstrated NRP1 also interacts with several heparin-binding growth factors, such as FGF-2, FGF-4 and HGF/SF, and potentiates the growth stimulatory activity of FGF-2 on endothelial cells (West *et al.*, 2005). As HGF/SF and FGF-2 were shown to stimulate cell growth through receptor-mediated autocrine signaling in glioma cells (Abounader and Laterra, 2005), we performed enzyme-linked immunosorbent assay (ELISA) and determined whether the autocrine signaling activities of these growth factors were involved in the NRP1-stimulated U87MG cell survival and growth. In a 48-h cell culture,

A

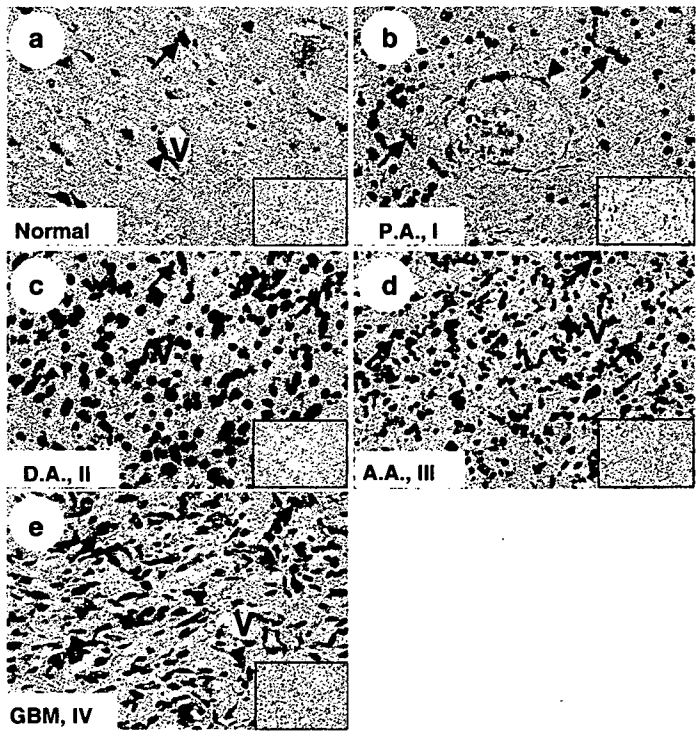

B **NRP-1 Expression Correlates with Human Glioma Progression**

WHO grade	n	Histology	n	Score -	±	1+	2+	3+	Kruskal-Wallis test* with Scheffe's post-hoc test
Normal	4	Normal	4	4	0	0	0	0	Normal+I
I	4	Pilocytic astrocytoma	4	0	4	0	0	0	Normal+I
II	24	Oligodendroglioma	13	2	4	5	2	0	II
		Diffuse astrocytoma	10	0	0	5	5	0	II
		Oligoastrocytoma	1	0	0	1	0	0	II
III	21	Anaplastic astrocytoma	13	0	1	7	5	0	III+IV
		Anaplastic oligodendroglioma	7	0	0	3	3	1	III+IV
		Anaplastic oligoastocytoma	1	0	0	0	1	0	III+IV
IV	43	Glioblastoma multiforme	43	0	3	16	18	6	III+IV

Normal+I vs II: $p < 0.01$; II vs III+IV: $p < 0.05$; Normal+I vs III+IV: $p < 0.01$

*Kruskal-Wallis test between Normal+Grade I vs Grade II vs Grade III+IV showed significant difference with $p < 0.00001$. Differences between each group were then examined by Scheffe's post-hoc test and each p-value were indicated in the table.

n, number of specimens. Score, intensity of IHC staining in the clinical specimens by an ant-NRP1-antibody and is defined as described in the Materials and Method section.

Figure 1 NRP1 expression correlates with human glioma progression. (**A**) IHC of paraffin sections of normal human brain (panel a), P.A. (WHO grade I, panel b), diffuse astrocytoma (D.A., grade II, panel c), anaplastic astrocytoma (A.A., grade III, panel d) and GBM (grade IV, panel e) tissue. Insets in panels a–e are the isotype-matched IgG control staining of identical areas. Arrows indicate neurons (a) or tumor cells (b to e) that are positive for NRP1. Arrowheads indicate endothelial cells in tumor-associated vessels that express NRP1. Results are representative of three independent experiments. Original magnification: × 400. (**B**) Statistical analyses. A total of 92 individual primary tumor specimens (WHO grade I–IV) and four normal human brain biopsies were analysed.

U87MG, LacZ and NRP1 cells secreted VEGF (30 ± 3.6 ng/ml/10^6 cells), FGF-2 (14 ± 2.1 pg/ml/10^6 cells) and HGF/SF (400 ± 45 pg/ml/10^6 cells) into serum-free medium at similar levels. A neutralizing anti-HGF/SF antibody abolished the effect of NRP1-enhanced U87MG cell survival, whereas neutralizing anti-FGF-2 and anti-VEGF antibodies had little or no effect on cell survival of U87MG and NRP1 cells (Figure 4B).

To investigate whether the HGF/SF/c-Met signaling pathway mediates NRP1 stimulation of glioma cells, we examined the expression and tyrosine phosphorylation

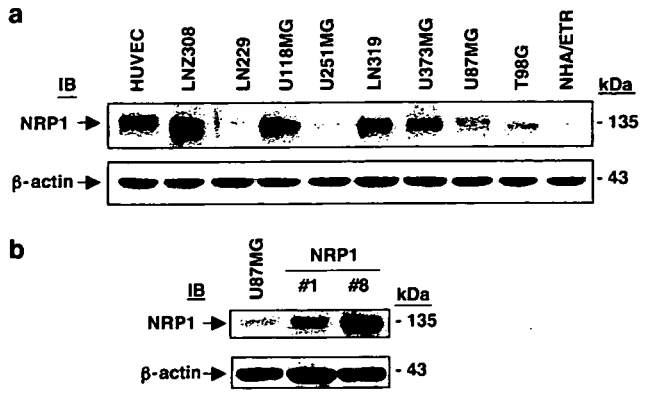

Figure 2 Overexpression of NRP1 in U87MG glioma cells. IB analyses of HUVEC, NHA/ETR and various glioma cell lines (**a**) or U87MG and NRP1-no. 1 and NRP1-no. 8 cells (**b**) using a polyclonal anti-NRP1 antibody (C-18). β-Actin was used as a loading control. Similar results were also obtained using a polyclonal anti-NRP1 antibody (NP1ECD1A). Results are representative of three independent experiments.

of c-Met in U87MG and NRP1 cells in the absence or presence of the HGF/SF neutralizing antibody. As shown in Figure 4C, in the absence of serum, expression of endogenous c-Met was not enhanced by NRP1 overexpression, but tyrosine phosphorylation of c-Met was stimulated in NRP1 but not U87MG or LacZ cells. When the HGF/SF neutralizing antibody was included in the cell culture, the NRP1-induced phosphorylation of c-Met was diminished. As U87MG, LacZ and NRP1 cells secrete low levels of endogenous HGF/SF in the serum-free CM (400 ± 45 pg/ml/10^6 cells) and no inhibitory effect of the neutralizing anti-HGF/SF on U87MG parental cell survival (Figure 4B) was seen, we reasoned that the HGF/SF/c-Met autocrine signaling pathway was not activated due to low levels of the endogenous HGF/SF in U87MG or LacZ cells. Furthermore, NRP1 overexpression in U87MG cells potentiated HGF/SF/c-Met autocrine signaling by activating a downstream target, Bad, an antiapoptotic molecule (Abounader and Laterra, 2005) (Figure 4C). Phosphorylation of Bad at Ser-112 was induced by NRP1 overexpression, but only a slight enhancement occurred on the constitutively phosphorylated Ser-136 of Bad. Additionally, a 4-day culture in serum-free medium did not alter the expression levels of NRP1 in U87MG, LacZ or NRP1-expressing cells (Figure 4D).

Although U87MG cells are deficient in plexin A1 and VEGFR-2, Sema 3A, a cognate ligand for NRP1, is expressed in U87MG cells (Rieger *et al.*, 2003). Thus, we tested a specific knockdown of Sema 3A by siRNA to examine the effects of endogenous Sema 3A on NRP1-enhanced U87MG cell growth. As shown in Figure 4E, endogenous c-Met (panel a) and Sema 3A (panel b) were considerably suppressed compared with the control siRNA-transfected cells. Reduced expression of c-Met, but not Sema 3A, in NRP1 cells significantly abolished the NRP1-enhanced U87MG cell survival (Figure 4F).

NRP1 potentiates glioma cell proliferation in response to exogenous HGF/SF

We assessed whether NRP1 overexpression could potentiate stimulation of glioma cell proliferation by exogenous HGF/SF using a BrdUrd incorporation assay. As shown in Figure 5A, in the absence of recombinant human (rh) HGF/SF, the basal level of BrdUrd incorporation in NRP1-no. 1 and -no. 8 cells was similar to that in U87MG and LacZ cells. When cells were treated with 5 or 10 ng/ml of rhHGF/SF, a significant increase in BrdUrd incorporation was found in NRP1-no. 1 and -no. 8 cells compared with U87MG and LacZ cells, whereas stimulation by 25 ng/ml rhHGF/SF markedly enhanced BrdUrd incorporation in U87MG and LacZ cells. Further increases of rhHGF/SF (50 or 75 ng/ml) had no further augmentation of BrdUrd incorporation in U87MG, LacZ and NRP1 cells. Also, NRP1-potentiated cell proliferation was proportional to the level of exogenous NRP1 expression in the glioma cells when comparing the BrdUrd incorporation level in NRP1-no. 8 cells (higher level of exogenous NRP1) to NRP1-no. 1 cells (lower level of NRP1 expression, Figure 2b).

Next, we assessed the activation of c-Met and two of its downstream effectors, ERK and Bad. As shown in Figure 5B, when cells were treated with 10 ng/ml rhHGF/SF for 20 or 40 min, phosphorylation of ERK1/2 and Bad at Ser-112 was evident in NRP1-expressing cells but not in LacZ cells. Moreover, treatment with 25 μmol/l U0126, a specific inhibitor for ERK, inhibited HGF/SF-stimulated phosphorylation of ERK and Bad as well as BrdUrd incorporation in NRP1 cells but not in LacZ cells (Figure 5Ca and b). To a similar extent, suppression of Bad protein expression in these cells by a specific siRNA (Figure 5Da) also significantly attenuated HGF/SF-stimulated BrdUrd incorporation in NRP1 cells but had no effect on LacZ cells or untreated cells (Figure 5Db).

To further confirm the critical role of NRP1 expression on potentiation of HGF/SF/c-Met signaling, we determined the effects of endogenous NRP1 on cell growth in LNZ-308 glioma cells, as LNZ-308 cells express endogenous NRP1 at high levels (Figure 2a) and no endogenous HGF/SF protein was detected by ELISA in serum-free CM (data not shown). As shown in Figure 6a, three individual siRNAs for NRP1 (N1, N2 and N3) suppressed endogenous NRP1 protein at various levels in LNZ-308 cells, whereas a pool of these three siRNAs for NRP1 (N1:N2:N3 = 1:1:1) considerably suppressed endogenous NRP1 protein. When control siRNA-transfected LNZ-308 cells were stimulated with rhHGF/SF, BrdUrd incorporation increased by 1.6-fold in response to 10 ng/ml of rhHGF/SF and reached a peak when 20 ng/ml HGF/SF was used (Figure 6b). Stimulation by HGF/SF on LNZ-308 cells at higher concentrations (60 and 80 ng/ml) had no further effect (Figure 6b). Importantly, when endogenous NRP1 expression was inhibited using siRNA, HGF/SF-stimulated BrdUrd incorporation at low concentrations (10 and 20 ng/ml) was significantly attenuated.

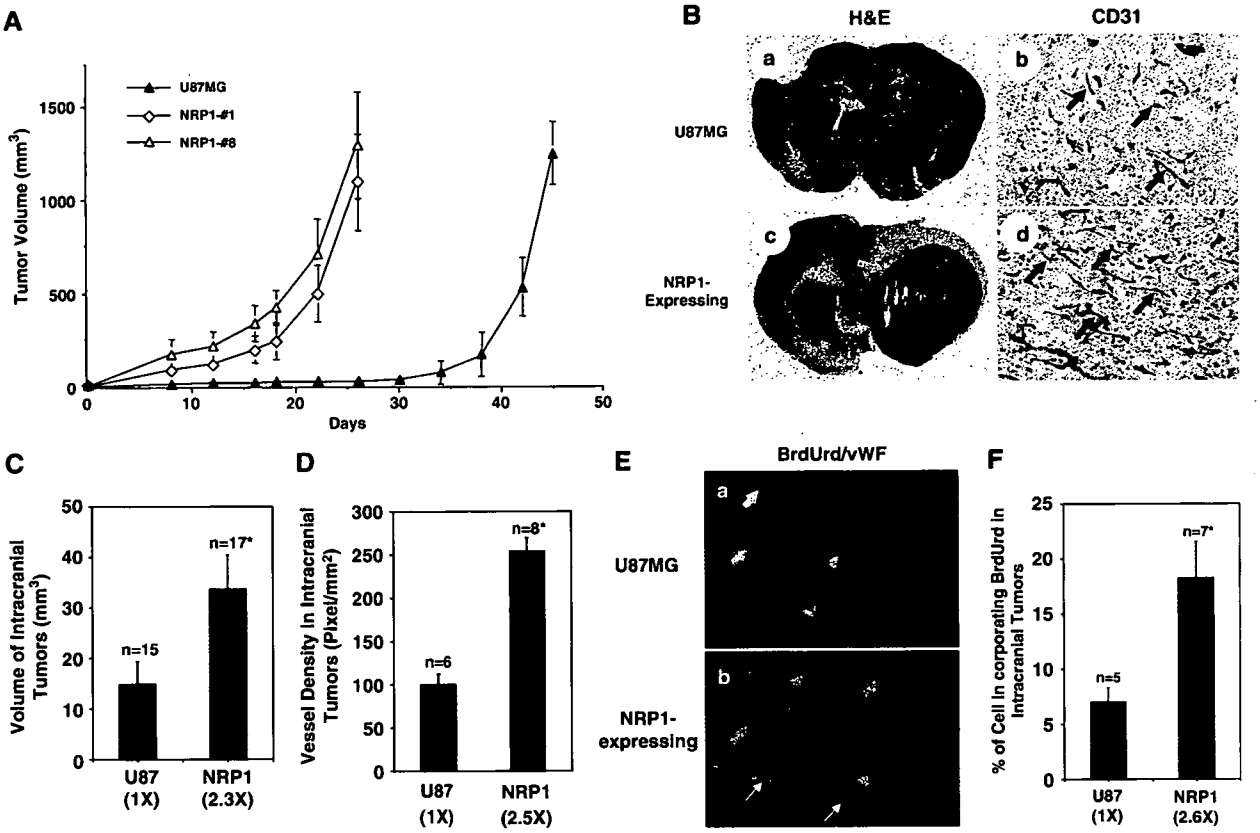

Figure 3 Overexpression of NRP1 in U87MG cells promotes tumor growth and angiogenesis. (**A**) Growth kinetics of U87MG or NRP1 tumors at subcutaneous sites. Tumor volume was estimated (volume $=(a^2 \times b)/2$, $a<b$) using a caliper at the indicated times. Data are shown as mean $\pm$ s.d. (**B**) Tumorigenicity and angiogenesis of U87MG brain tumors. IHC analyses are shown for U87MG (panels a and b) or NRP1 (c and d) gliomas. Panels a and c are brain sections stained with hematoxylin and eosin (H&E). Panels b and d show CD31 staining for tumor vessels. Arrows in a and c, tumor mass. Arrows in b and d, blood vessels. Five to eight individual tumor samples of each group from each *in vivo* experiment were analysed. Original magnification: panels a and c, $\times$ 12.5; b and d, $\times$ 200. (**C**) and (**D**) Quantitative analyses of tumorigenesis and angiogenesis in various intracranial tumors. Data are means $\pm$ s.d. Numbers in parentheses, the difference in fold between U87MG and NRP1 gliomas. (**E**) and (**F**) Cell proliferation of various intracranial gliomas. (**E**) IHC staining of U87MG brain tumors with a monoclonal anti-BrdUrd antibody (red) together with a polyclonal anti-vWF antibody (green). Blue arrows, proliferative nuclei in tumor cells. White arrows, proliferative nuclei of blood vessels. Blue arrowheads, vWF staining of vessels. Three to five serial sections from five to seven individual samples of each tumor type were analysed. Original magnification: $\times$ 400. (**F**) Quantitative analyses of cellular BrdUrd incorporation in U87MG and U87MG/NRP1 tumors. Numbers in parentheses, the difference in fold between U87MG/NRP1 and parental U87MG gliomas. Results in (**A–E**) are representative of three independent experiments.

Next, we examined activation of the HGF/SF/c-Met signaling pathway in various siRNA-transfected LNZ-308 cells in response to HGF/SF stimulation. As shown in Figure 6c, HGF/SF stimulation at 10, 25 and 50 ng/ml induces phosphorylation of c-Met, Erk1/2 and Bad. When NRP1 expression was suppressed using siRNA, the activation by HGF/SF at 10 and 25 ng/ml on c-Met, ERK1/2 and Bad was diminished. No inhibitory effect on HGF/SF stimulation was seen when NRP1 siRNA-transfected LNZ-308 cells were treated with 50 ng/ml HGF/SF.

NRP1 enhances HGF/SF/Met signaling in human glioma

Next, we sought to determine whether activation of c-Met also occurred in NRP1-expressing tumors *in vivo*. We extracted tissue lysates from U87MG and NRP1 tumors and performed IB analysis. As shown in Figure 7a, NRP1 overexpression did not increase c-Met expression in the NRP1 tumors. However, increased phosphorylation of c-Met was detected in the tissue lysates of NRP1 tumors compared with the parental tumors established at subcutaneous and orthotopic sites. Finally, we examined whether increased expression of NRP1 and c-Met phosphorylation correlates with glioma progression in 14 primary human glioma tissue samples by IB analyses. As shown in Figure 7b, c-Met was detected at various levels in all of the glioma tissues, whereas upregulation of NRP1 expression was seen primarily in high-grade tumors (grades III and IV). Importantly, c-Met phosphorylation was also increased in high-grade gliomas, mostly in grade IV GBM specimens, correlating with the expression profile of NRP1 in these clinical samples.

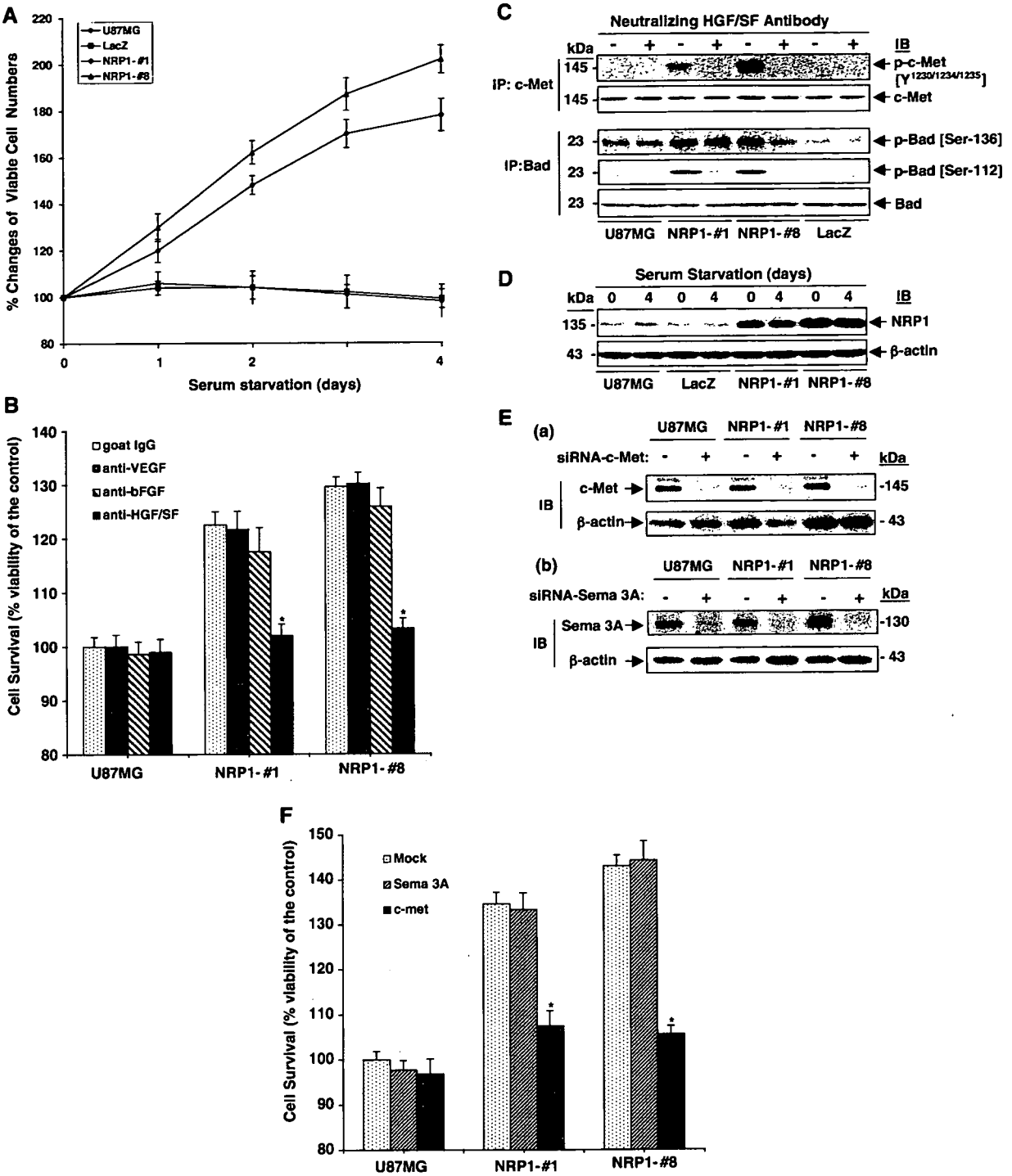

Figure 4 NRP1 promotes survival of U87MG cells by enhancing autocrine HGF/SF/c-Met signaling. (**A**) Overexpression of NRP1 promotes U87MG cell survival. Data of cell survival assays are shown as mean ± s.d. (**B**) Inhibition of HGF/SF, but not FGF-2 or VEGF, suppresses NRP1-promoted U87MG cell survival. Data of cell survival assays are shown as mean ± s.d. (**C**) Inhibition of tumor cell-derived HGF/SF, but not VEGF or FGF-2, suppresses NRP1-potentiated activation of c-Met and Bad. IP and IB analyses of various U87MG cells treated with or without the HGF/SF neutralizing antibody. (**D**) Serum starvation did not alter NRP1 expression in U87MG, LacZ and NRP1 cells. IB analyses of various cell lysates under the same conditions as in (**A**). (**E**) and (**F**) Inhibition of endogenous c-Met but not Sema 3A attenuates NRP1-potentiated U87MG cell viability. (**E**) Suppression of endogenous c-Met and Sema 3A by siRNA. IB analyses of c-Met and Sema 3A proteins in various U87MG cells. (**F**) Cell survival assays of siRNA-transfected U87MG and NRP1 cells. Data are shown as mean ± s.d. In (**B–D**), c-Met, Bad and β-actin were used as loading controls. Results in (**A–F**) are representative of three independent experiments.

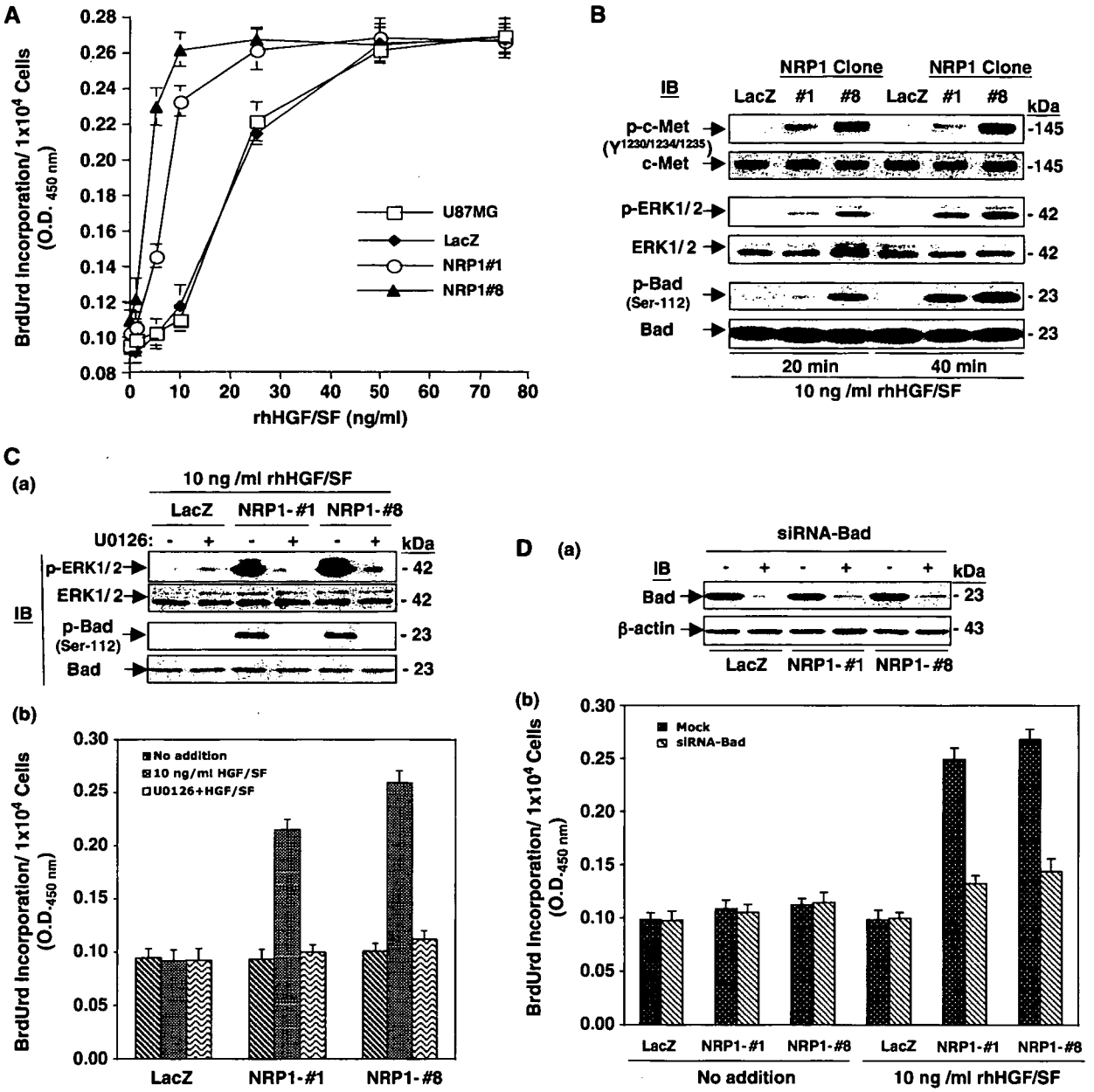

Figure 5 NRP1 expression potentiates HGF/SF stimulation of cell proliferation mediated by c-Met signaling. (**A**) Expression of NRP1 in U87MG cells potentiates cell proliferation in response to a low dose of HGF/SF stimulation. Data of BrdUrd incorporation in U87MG, LacZ, NRP1-no. 1, and NRP1-no. 8 cells are shown as mean±s.d. (**B**) IB analyses of NRP1-potentiated HGF/SF stimulation of phosphorylation on c-Met, ERK1/2 and Bad in various U87MG cells. (**C**) U0126 attenuated NRP1-potentiated HGF/SF stimulation of phosphorylation on ERK1/2 and Bad (panel a, IB analyses) and cell proliferation in various U87MG cells (panel b, BrdUrd incorporation assays; data are shown as mean±s.d.). (**D**) Knockdown of Bad by siRNA (panel a, IB analyses) attenuates NRP1-potentiated HGF/SF stimulation of cell proliferation in various U87MG cells (panel b, data are shown as mean±s.d.). In (**B–D**), c-Met, ERK1/2, Bad and β-actin were used as loading controls. Results in (**A**) to (**D**) are representative of three independent experiments.

Discussion

The role of NRP1 in human tumor progression has been studied in various cancer model systems. Upregulation of NRP1 was found not only in endothelia but also in tumor cells in various types of primary human cancer specimens (Ding *et al.*, 2000; Akagi *et al.*, 2003). Overexpression of NRP1 in tumor cells has been shown to promote tumor growth and angiogenesis in xenograft models and cell survival in cancer cells. In these reports, NRP1 stimulation of tumor progression was primarily attributed to VEGF-dependent pathways (Miao *et al.*, 2000; Bachelder *et al.*, 2003). This study provides new evidence that glioma cell-expressed NRP1 promotes tumor progression through potentiating the HGF/SF/c-Met signaling pathway. We show in primary human

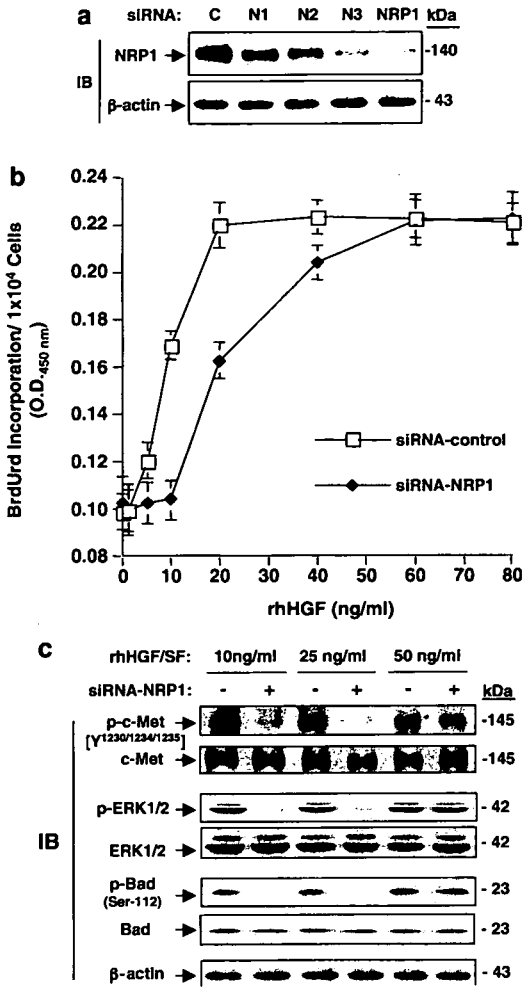

Figure 6 Inhibition of endogenous NRP1 attenuated HGF/SF stimulation of cell proliferation and HGF/SF/c-Met signaling in LNZ-308 glioma cells. (**a**) Inhibition of endogenous NRP1 by NRP1/siRNA in LNZ-308 cells detected by IB analyses. C, control siRNA. N1, N2 and N3, individual siRNAs for NRP1. NRP1, a pool of all three siRNAs of N1, N2 and N3. β-Actin was used as a loading control. (**b**) Inhibition of endogenous NRP1 in LNZ-308 cells using siRNA-attenuated rhHGF/SF stimulation of cell proliferation. Data of BrdUrd incorporation of siRNA-transfected LnZ-308 cells are shown as mean ± s.d. (**c**) Inhibition of endogenous NRP1 in LNZ-308 cells using siRNA-suppressed HGF/SF stimulation of c-Met signaling detected by IB analyses. c-Met, ERK1/2 Bad and β-actin were used as loading controls. Results in (**a–c**) are representative of three independent experiments.

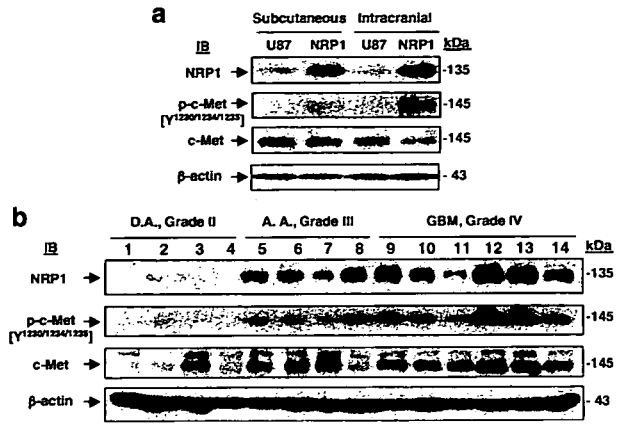

Figure 7 Upregulation of NRP1 correlates with the activation of c-Met in U87MG tumor xenografts and in high-grade human glioma specimens. (**a**) Overexpression of NRP1 in U87MG xenografts resulted in activation of c-Met in the established tumors. IB analyses of U87MG and NRP1 xenografted tumors. β-Actin was used as a loading control. (**b**) Upregulation of NRP1 expression correlates with activation of c-Met during glioma progression. IB analyses of 14 frozen primary human glioma specimens. c-Met and β-actin were used as loading controls. Results are representative of three independent experiments.

glioma specimens that upregulation of tumor cell-expressed NRP1 correlates with glioma progression and increased activation of c-Met in these clinical tumor samples. We demonstrated that overexpression of NRP1 by U87MG glioma cells enhanced tumor growth in mice through potentiating HGF/SF/c-Met activity stimulating tumor cell proliferation in mice. NRP1 potentiated the autocrine HGF/SF/c-Met signaling pathway in response to low concentrations of HGF/SF *in vitro*, and NRP1 expression is also correlated with c-Met activation in U87MG tumors that overexpress NRP1. Conversely, inhibition of tumor cell-derived HGF/SF, but not FGF-2 or VEGF, by neutralizing antibodies and of endogenous c-Met, but not Sema 3A, by specific siRNAs attenuates HGF/SF/c-Met signaling and glioma cell viability. Furthermore, suppression of endogenous NRP1 in LNZ-308 cells abolishes exogenous HGF/SF stimulation of c-Met-mediated signaling in the tumor cells at lower concentrations. Our results corroborate a recent study showing that overexpression of NRP1 in human pancreatic cancer cells resulted in constitutive activation of mitogen-activated protein kinase signaling (Wey *et al.*, 2005). A plausible mechanism of NRP1 stimulation of tumor progression in our study and the pancreatic cancer model is that NRP1 enhances endogenous signaling modulating tumor cell function independent of VEGF. Our results of NRP1 potentiation of the HGF/SF/c-Met signaling pathway in glioma cells agree with another recent study showing that that NRP1 not only interacts directly with multiple heparin-binding growth factors, such as FGF-2, FGF-4 and HGF/SF, but also potentiates stimulation of FGF-2 on endothelial cells (West *et al.*, 2005). In addition, the increased sensitivity to HGF/SF/c-Met signaling by endogenously expressed NRP1 in glioma cells is analogous to the increase in sensitivity to FGF-2 caused by the addition of a soluble NRP1 dimer to endothelial cells in the aforementioned study. Expression of NRP1 in various cell types may sensitize the cells to their microenvironments, thereby potentiating the corresponding intracellular signaling critical for cellular function.

Increased expression of NRP1 has been detected in tumor cells in clinical glioma samples, suggesting a link between NRP1 expression and glioma malignancy (Ding *et al.*, 2000). Our results further elaborate on these observations. By analysing a total of 92 primary human

glioma specimens, we show that upregulation of NRP1 in tumor cells correlates with glioma progression. In U87MG tumor xenografts, overexpression of NRP1 markedly stimulated angiogenesis at both anatomic sites (Figure 3). Significant stimulation of vessel growth by tumor cell–expressed NRP1 in our U87MG xenografts and in prostate and colon cancer models (Miao *et al.*, 2000) led to a hypothesis that tumor cell-expressed NRP1 stimulates vessel growth through a juxtacrine mechanism that forms a complex of NRP1 (in tumor cells), VEGF within the tumor microenvironment (intercellular) and VEGFR-2 (in endothelial cells), thus potentiating VEGF activity that enhances angiogenesis and tumor growth (Klagsbrun *et al.*, 2002). However, it is difficult to dissect the NRP1-stimulated juxtacrine signaling in harvested tumor tissues. Nonetheless, these data and the aforementioned studies suggest a far wider spectrum of activity of NRP1 in promoting tumor progression than is currently appreciated.

In summary, this study provides a novel mechanism that expression of NRP1 in human glioma cells promotes glioma progression through potentiating the activity of HGF/SF/c-Met autocrine pathways. Upregulation of NRP1 in tumor cells correlates with the activation of HGF/SF/c-Met pathways in both primary glioma specimens and xenograft gliomas, and inhibition of endogenous c-Met or NRP1 attenuates NRP1-enhanced HGF/SF/c-Met signaling. In addition, our data demonstrating NRP1 expression patterns in primary human glioma specimens and significant enhancement of tumor angiogenesis in glioma xenografts suggest that tumor cell-derived NRP1 stimulates vessel growth in a juxtacrine manner. These pathways appear to act in concert in promoting glioma growth and angiogenesis. Thus, our studies demonstrate a necessity for simultaneously targeting NRP1/VEGF and HGF/SF/c-Met signaling pathways in the treatment of human gliomas.

Materials and methods

Cell lines and their cultures

Human glioma cell lines U87MG, U118MG and T98G were obtained from the American Type Culture Collection (Manassas, VA, USA). Human glioma cell lines U251MG, U373MG, LNZ-308, LN229 and LN319 were from our collection. The transformed normal human astrocytes that form WHO grade III-like glioma in the murine brain (NHA/ETR) were from Dr R Pieper. Human umbilical endothelial cells (HUVEC) were from Cambrex (Rockland, ME, USA). The cells were cultured as described previously (Guo *et al.*, 2001).

siRNA transient transfection

siRNAs were synthesized by Dharmacon Inc. (Lafayette, CO, USA). The sequences of siRNA for target genes were Met, 5′-GTGCAGTATCCTCTGACAG-3′; Sema 3A, 5′-AAAGTTC ATTAGTGCCCACCT-3′ and NRP1 N1, 5′-GAGAGGTCC TGAATGTTCC-3′, N2, 5′-AAGCTCTGGGCATGGAATC AG-3′, and N3, 5′-AAAGCCCCGGGTACCTTACAT-3′; and Bad, Signal Silence Bad siRNA kit (Cell Signaling, Beverly, MA, USA). Cells were transfected with 120 nM of the indicated siRNA or a control siRNA (Invitrogen) using the Oligofectamine reagent (Invitrogen Inc., Carlsbad, CA, USA). After 24 h, siRNAs were removed and the cells were maintained in medium containing 10% FBS for an additional 48 h. The inhibition of protein expression was assessed by IB analysis.

Other methods

Reagents, antibodies, analyses of primary human glioma specimens, IHC, statistics, glioma xenograft models, immunoprecipitation (IP), IB, *in vivo* BrdUrd labeling, generation of U87MG NRP1-expressing cell lines and cell survival and proliferation assays are described in the Supplementary Information.

Acknowledgements

The work was supported by grants NIH CA102011 and RSG CSM-107144 (S-Y C), the Hillman Fellows Program for Innovative Cancer Research to S-Y C and B H, and grant NIH CA095809 to TM (in part).

References

Abounader R, Lal B, Luddy C, Koe G, Davidson B, Rosen EM *et al.* (2002). *In vivo* targeting of SF/HGF and c-met expression via U1snRNA/ribozymes inhibits glioma growth and angiogenesis and promotes apoptosis. *FASEB J* **16**: 108–110.

Abounader R, Laterra J. (2005). Scatter factor/hepatocyte growth factor in brain tumor growth and angiogenesis. *Neuro-oncol* **7**: 436–451.

Akagi M, Kawaguchi M, Liu W, McCarty MF, Takeda A, Fan F *et al.* (2003). Induction of neuropilin-1 and vascular endothelial growth factor by epidermal growth factor in human gastric cancer cells. *Br J Cancer* **88**: 796–802.

Bachelder RE, Lipscomb EA, Lin X, Wendt MA, Chadborn NH, Eickholt BJ *et al.* (2003). Competing autocrine pathways involving alternative neuropilin-1 ligands regulate chemotaxis of carcinoma cells. *Cancer Res* **63**: 5230–5233.

Bagri A, Tessier-Lavigne M. (2002). Neuropilins as Semaphorin receptors: *in vivo* functions in neuronal cell migration and axon guidance. *Adv Exp Med Biol* **515**: 13–31.

Ding H, Wu X, Roncari L, Lau N, Shannon P, Nagy A *et al.* (2000). Expression and regulation of neuropilin-1 in human astrocytomas. *Int J Cancer* **88**: 584–592.

Gagnon ML, Bielenberg DR, Gechtman Z, Miao HQ, Takashima S, Soker S *et al.* (2000). Identification of a natural soluble neuropilin-1 that binds vascular endothelial growth factor: *in vivo* expression and antitumor activity. *Proc Natl Acad Sci USA* **97**: 2573–2578.

Gao CF, Vande Woude GF. (2005). HGF/SF-Met signaling in tumor progression. *Cell Res* **15**: 49–51.

Guo P, Xu L, Pan S, Brekken RA, Yang ST, Whitaker GB *et al.* (2001). Vascular endothelial growth factor isoforms display distinct activities in promoting tumor angiogenesis at different anatomic sites. *Cancer Res* **61**: 8569–8577.

Hu B, Guo P, Fang Q, Tao HQ, Wang D, Nagane M *et al.* (2003). Angiopoietin-2 induces human glioma invasion through the activation of matrix metalloprotease-2. *Proc Natl Acad Sci USA* **100**: 8904–8909.

Klagsbrun M, Takashima S, Mamluk R. (2002). The role of neuropilin in vascular and tumor biology. *Adv Exp Med Biol* **515**: 33–48.

Laterra J, Rosen E, Nam M, Ranganathan S, Fielding K, Johnston P. (1997). Scatter factor/hepatocyte growth factor expression enhances human glioblastoma tumorigenicity and growth. *Biochem Biophys Res Commun* **235**: 743–747.